sPH-TRG-2022-00X

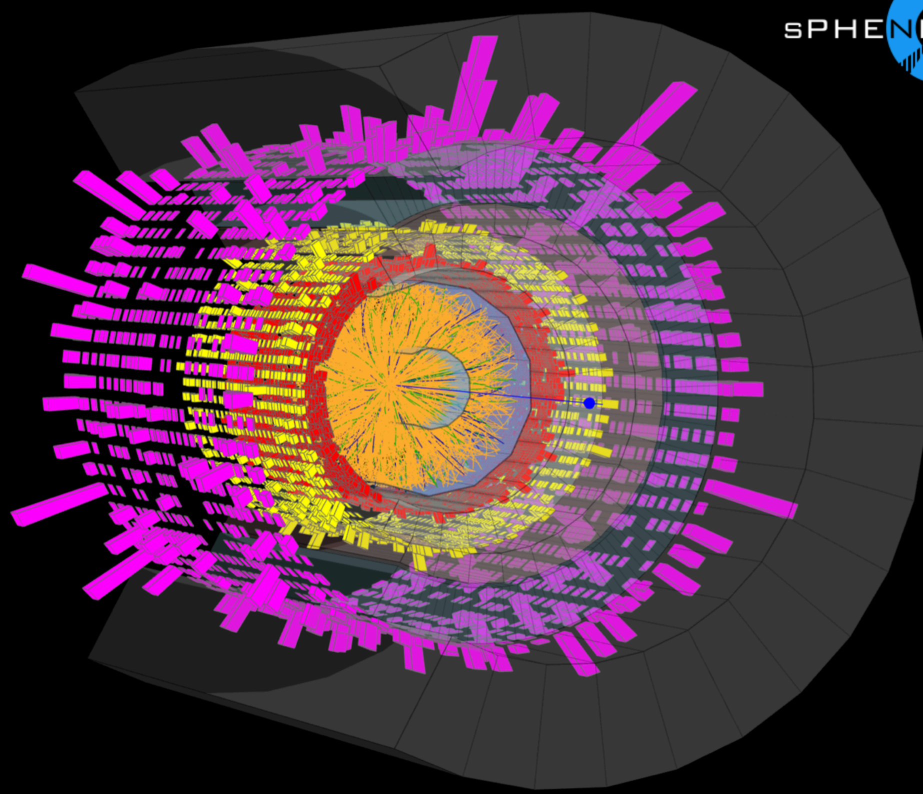

sPHENIX Beam Use Proposal

May 7, 2022

DRAFT for Internal Collaboration Review

Executive Summary

sPHENIX will be the first new collider detector at RHIC in over twenty years with new measurement capabilities that have not previously available in this energy range. The experiment is a specific priority of the DOE/NSF NSAC 2015 Nuclear Physics Long Range Plan, and the significance of its expected results, complementing those coming from the LHC, was highlighted in the "Working Group 5: Heavy-Ion" input to the European Strategy for Particle Physics. sPHENIX will play a critical role in the completion of the RHIC science mission by enabling qualitatively new measurements of the microscopic nature of quark-gluon plasma. These studies rely on very high statistics measurements of jet production and substructure, and open and hidden heavy flavor over an unprecedented kinematic range at RHIC. They are enabled by the high rate and large acceptance of the detector, combined with precise tracking and electromagnetic and hadronic calorimetry.

The effort to construct the experiment is officially underway with the DOE Major Item of Equipment (MIE) project having been granted PD-2/3 approval in September 2019. Additional subdetectors are also under construction and will be integrated into the full experiment, completing its science capabilities. These are funded as Brookhaven National Laboratory capital projects (e.g., the micro-vertex detector, MVTX), or realized as contributions from collaborating institutions (e.g., the intermediate silicon strip tracker, INTT). The sPHENIX resource-loaded schedule leads to a first year of operation in 2023; the final year of sPHENIX data taking in 2025 is dictated by Brookhaven's reference schedule for the Electron Ion Collider (EIC) project. This document responds to a charge (see Appendix A) from the BNL NPP Associate Laboratory Director (ALD) to detail the sPHENIX run plan during the years 2023–2025.

In the run plan described in this document, each of the three years plays a critical role in fulfilling the science mission outlined in the Nuclear Physics Long Range Plan:

- Year-1 (2023) serves to commission all detector subsystems and full detector operations, and to validate the calibration and reconstruction operations essential to delivering the sPHENIX science in a timely manner. Close coordination with C-AD will be required in the ramp-up of RHIC luminosity and optimization of beam operations to achieve these goals in a safe manner, enabling full exploitation of RHIC luminosity in Year-2 and Year-3. Year-1 will also allow collection of a Au+Au data set enabling sPHENIX to repeat and extend measurements of "standard candles" at RHIC.

- Year-2 (2024) will see commissioning of the detector for p+p collisions and collection of large p+p and p+Au data sets. These are critical as reference data for the Au+Au physics and, due to the transverse polarization of the proton beams, for substantial new studies of cold QCD physics. We highlight that a modest streaming readout upgrade of the tracking detectors

Table 1: Summary of the sPHENIX Beam Use Proposal for years 2023–2025, as requested in the charge. The values correspond to 24 cryo-week scenarios, while those in parentheses correspond to 28 cryo-week scenarios. The 10%-*str* values correspond to the modest streaming readout upgrade of the tracking detectors. Full details are provided in Chapter 2.

Year	Species	$\sqrt{s_{NN}}$ [GeV]	Cryo Weeks	Physics Weeks	Rec. Lum. $\lvert z\rvert$ <10 cm	Samp. Lum. $\lvert z\rvert$ <10 cm
2023	Au+Au	200	24 (28)	9 (13)	3.7 (5.7) nb^{-1}	4.5 (6.9) nb^{-1}
2024	$p^{\uparrow}p^{\uparrow}$	200	24 (28)	12 (16)	0.3 (0.4) pb^{-1} [5 kHz] 4.5 (6.2) pb^{-1} [10%-*str*]	45 (62) pb^{-1}
2024	$p^{\uparrow}$+Au	200	–	5	0.003 pb^{-1} [5 kHz] 0.01 pb^{-1} [10%-*str*]	0.11 pb^{-1}
2025	Au+Au	200	24 (28)	20.5 (24.5)	13 (15) nb^{-1}	21 (25) nb^{-1}

[10%-*str*], requiring no additional hardware, will greatly extend this physics program in p+p and p+Au running.

- Year-3 (2025) is focused on the collection of a very large Au+Au data set for measurements of jets and heavy flavor observables with unprecedented statistical precision and accuracy.

Table 1 provides an overview of the data we expect to obtain in Year-1 to Year-3 (2023 - 2025), as requested in the ALD charge. The total Au+Au data set from this three-year proposed running, in the 28 cryo-week scenario, is equivalent to 141 billion events recorded for all physics analyses.

This document is organized as follows. Chapter 1 provides a brief summary of the sPHENIX physics program and status of the sPHENIX project. Chapter 2 details the Year-1 to Year-3 (2023-2025) Beam Use Proposal from sPHENIX including a break down in terms of cryo-weeks. Chapters 3 discusses the commissioning plan for sPHENIX. Chapter 4 presents the physics projections and deliverables from the Year-1 to Year-3 Beam Use Proposal. We highlight that the full sPHENIX physics case is described in the original sPHENIX proposal, and here we focus on demonstrating that within this Beam Use Proposal those physics goals can be achieved. Chapter 5 provides a brief summary.

Additional information which may be of interest is included in the appendices. Appendix A contains the BUP charge from the ALD. Appendix B further details inputs to the luminosity projections from C-AD. Appendix C documents modest upgrades to sPHENIX for the streaming readout capability. Finally, in Appendix D we outline a potential plan for additional running in Year-4 to Year-5 (2026 - 2027), should the occasion arise. This would provide unique opportunities for collecting massive, archival Au+Au and spin polarized p+p data sets in the final years of RHIC operation, in addition to new geometry combinations (such as O+O and Ar+Ar).

Contents

Chapter 1

sPHENIX overview

1.1 Science mission

Over the last decades, experiments at RHIC and LHC have shown that collisions of heavy nuclei produce a hot and dense state of matter, called Quark-Gluon Plasma (QGP). These studies demonstrated that the QGP is unique among all forms of matter in terms of its viscosity η/s, opacity and vorticity. The QGP is a key example of a class of strongly coupled systems found recently in a wide range of areas of physics, from string theory to condensed matter and ultra-cold atom systems.

While measurements have provided detailed knowledge of the QGP's macroscopic (long wavelength) properties, we do not yet understand how these properties arise from the fundamental interactions of its constituents, i.e., quarks and gluons governed by the laws of Quantum Chromodynamics (QCD). In the 2015 Hot QCD Whitepaper [1] and the US Nuclear Physics Long Range Plan (LRP) [2], one of two highest priority goals in the field of Hot QCD was described as "Probe the inner workings of QGP by resolving its properties at shorter and shorter length scales. The complementarity of the two facilities [i.e., RHIC and LHC] is essential to this goal, as is a state-of-the-art jet detector at RHIC, called sPHENIX" [2].

To elucidate the nature of the QGP, the sPHENIX physics program rests on measurements using hard probes that are sensitive to the QGP microscopic structure over a broad range of length or momentum scales. These measurements at the top RHIC energy of $\sqrt{s_{NN}} = 200$ GeV include in particular studies of jet production and substructure, quarkonium suppression and open heavy flavor production and correlations. The sPHENIX studies will complement those planned at LHC for Run 3 during high luminosity Pb+Pb operations and provide qualitative improvements over current measurements at RHIC for related observables. While the existing RHIC measurements have greatly contributed to our understanding of the QGP, the overall kinematic range for many jet and photon+jet observables is constrained to $p_T < 20$ GeV even for the highest statistics measurements and therefore insufficient for a direct comparison to LHC studies. In contrast, the projected sPHENIX measurements reach sufficiently high p_T to provide a significant overlap with the low range of measurements at the LHC, allowing to study identical hard probes embedded into QGP with different initial conditions and expansion dynamics.

sPHENIX was proposed by the PHENIX collaboration in their 2010 Decadal Plan as an upgrade

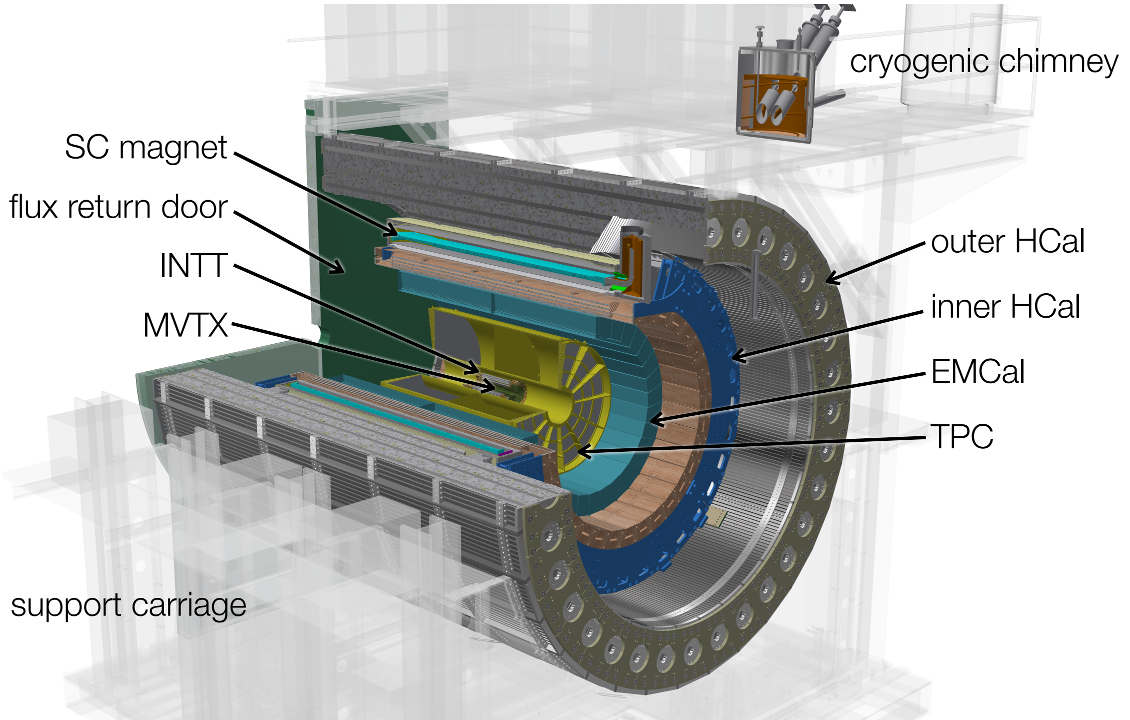

Figure 1.1: Engineering drawing (cutaway) of the sPHENIX detector. From the inside out the drawing shows tracking system, electromagnetic calorimeter and inner hadronic calorimeter, superconducting magnet and outer hadronic calorimeter. A detailed discussion of the sPHENIX detector subsystems can be found in the sPHENIX Technical Design Report [3]

(or replacement) of the PHENIX experiment at RHIC. The physics case and detector design were further developed in the years leading up to the 2015 Nuclear Physics LRP. A detailed design proposal was completed in 2015 [4], and in early 2016 the current sPHENIX collaboration was formed. As of early 2020, sPHENIX has more than 320 members from 80 institutions in 13 countries. The project received DOE CD-0 approval in late 2016, CD-1/3a approval in 2018 and entered its construction phase after PD 2/3 approval in fall 2019. The schedule foresees commissioning of the detector in 2022 and start of physics data taking in early 2023. The current expectation for 2025 as the final year of sPHENIX operations is dictated by BNL's reference schedule for the EIC project.

1.2 sPHENIX performance measures

The layout of the sPHENIX detector is shown in Figure 1.1. The experiment has been designed to allow high-statistics, high-resolution measurements for a broad range of observables related to jet production and modification, quarkonium production at high mass (or high p_T), and yields and correlations of heavy quark (charm and bottom) hadrons and heavy flavor tagged jets. This is achieved through several advances compared to the current instrumentation at RHIC:

- High data rates: the sPHENIX tracking and calorimetry provide hermetic coverage over full azimuth and pseudorapidity $|\eta| < 1$, with a readout rate of 15 kHz for all subdetectors.

The detector also provides triggering capabilities in $p+p$, and for selected observables in Au+Au, as well as the option for streaming readout of the tracking detectors. In combination, statistical precision compared to the current status at RHIC will improve by 1-2 orders of magnitude for many observables.

- High resolution vertexing: the MAPS-based micro-vertex detector, MVTX, provides larger acceptance, faster readout and higher resolution compared to previous RHIC detectors, enabling a state-of-the-art open heavy flavor program, including a large set of b-hadron measurements.

- Hadronic calorimetry: as a first at RHIC, sPHENIX features large acceptance hadronic calorimetry, enabling unbiased selection (and triggering in $p+p$) for jets, as well as improving the jet energy resolution and extending the range for high-p_T single hadron measurements through the rejection of mis-reconstructed tracks. In combination with the MVTX, this will allow the first application of b-jet tagging at RHIC.

1.3 The sPHENIX Project

The sPHENIX detector is being realized via several projects that are coordinated under a common project management structure. There are the elements of the original DOE Major Item of Equipment (MIE) — the outer hadronic calorimeter (oHCal), the central rapidity portion of electromagnetic calorimeter (EMCal) covering $|\eta| < 0.85$, the time projection chamber (TPC), and their associated readout electronics and services. A silicon strip tracker (INTT) is being provided by RIKEN. Additional tungsten/scintillating fiber blocks extending the coverage of the EMCal to $|\eta| < 1.1$ are being provided by a consortium of collaborating institutions. The inner longitudinal section of the hadronic calorimeter (iHCal) and the silicon pixel vertex detector (MVTX) are being pursued as BNL capital projects. The sPHENIX event plane detector (sEPD) is funded by an National Science Foundation (NSF) Major Research Instrument (MRI) grant. A quartz Čerenkov minimum bias detector, originally built by Hiroshima University for the PHENIX experiment, is being re-purposed for use in sPHENIX. There are also BNL funded projects to upgrade the infrastructure at IP8, to operate the 1.5 T BaBar superconducting solenoid, and to integrate and install the sPHENIX detector into the IP8 area. A labeled depiction of the main elements of the sPHENIX detector is shown in Figure 1.1.

The sPHENIX MIE received Critical Decision CD-1/3A approval in August 2018. A memo from DOE that same summer specified that projects below $50M would no longer be managed under DOE Order 413.3B, but would instead be managed by the Laboratories, the details of which were to be worked out between the National Laboratories and DOE. The end result was that sPHENIX would be working toward Project Decisions (PDs), to be approved by the BNL Laboratory Director with DOE concurrence. sPHENIX received PD-2/3 approval in September 2019, and has undergone regular Cost & Schedule reviews. The MIE has an early completion date of November 2021 and a PD-4 date of December 2022. The PD-4 goal is to provide a detector at RHIC ready to take commissioning data with collisions.

1.4 Elements of the Project

The full sPHENIX project consists of a large number of different elements, some of which are a DOE major Item of Equipment (MIE) project, others are part of an upgrade to the infrastructure in Bldg. 1008, others are BNL capital projects, and others are contributions from collaborating institutions. It is beyond the scope of this document to describe all aspects of the project in great detail; instead we will focus on the significant progress that has been made with detector elements since the last NPP Program Advisory Committee meeting.

1.4.1 MIE

The MIE scope consists of six detector projects and management of the MIE and related projects. The detector systems are:

- The compact (80 cm radius), ungated Time Projection Chamber (TPC), with GEM-based readout digitized via modified SAMPA ASICs, which were developed for the ALICE experiment
- The electromagnetic calorimeter, a tungsten-scintillating fiber SPACAL read out with solid state photomultiplier (SiPM's)
- The outer hadronic calorimeter, tilted steel plates with scintillating tiles interspersed in slots, also read out with SiPMs, which also doubles as the flux return of the 1.5 T superconducting solenoid
- Common electronics to read out both calorimeters consisting of shaper amplifiers on the detector which bring analog signals to 60 MHz waveform digitizers outside the solenoid
- Data acquisition designed to be capable of taking minimum bias Au+Au collisions at 15 kHz with greater than 90% livetime, and minimum bias triggers for Au+Au collisions, and jet and photon triggers for p+p and p+A operation
- The Minimum Bias Detector (MBD), which consists of the refurbished PHENIX Beam-Beam Counter (BBC), read out and triggered with new electronics based on the digitizers designed for the calorimeters

The detector systems range from having finished construction and installation to being well under way. The TPC and calorimeter prototypes have been tested in beam at Fermilab.

The TPC inner field cage, shown in Figure 1.2, has been completed at SBU. The modified SAMPA ASIC (V5, with a shorter shaping time to reduce pileup effects) has been prototyped, characterized, manufactured in quantity sufficient for the detector, and production testing is ongoing at Lund University. Production of all EMCal calorimeter blocks at the University of Illinois Urbana-Champaign (UIUC) is complete, and all sectors have now been assembled and instrumented at BNL. Figure 1.3 shows the modules with light guides and readout mounting (left) and the assembled EMCal Sector "0" (right). All 32 sectors of Outer HCal have been assembled and instrumented at BNL and installed in the experimental hall atop the carriage and cradle, surrounding the magnet, as can be seen in Figure 1.4 (left). Prototype electronics for the MBD have demonstrated time resolution that exceeds the requirements.

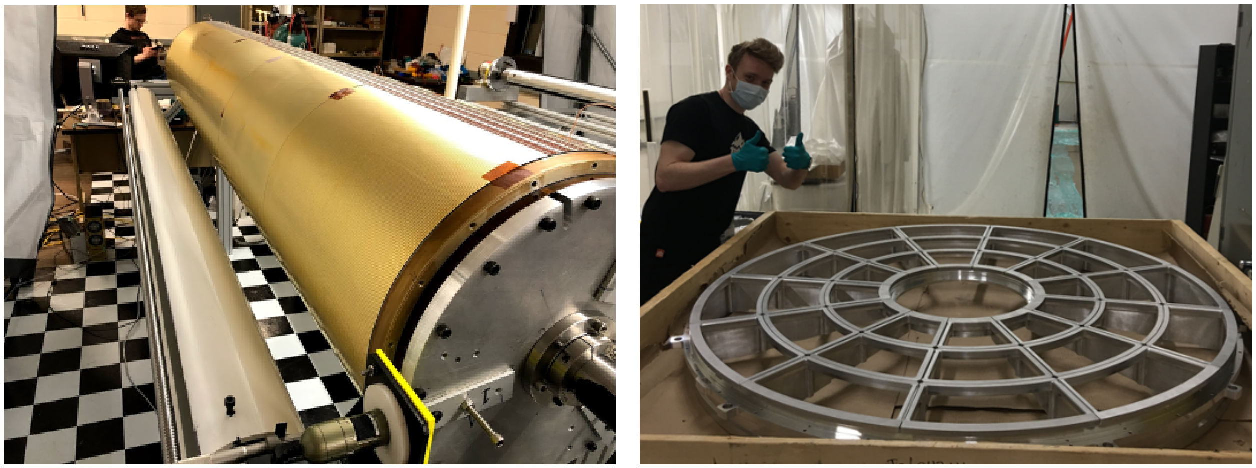

Figure 1.2: (left) The inner field cage of the TPC. A length of PVC sewer pipe, milled to a precise outer diameter, was used as an economical form upon which the field cage was built. (right) One of the two TPC "wagon wheels" which supports the TPC field cages, the GEMs, the readout electronics and all the services. The wheels are each milled from a single billet of aluminum improving the gas tightness of the TPC by eliminating a large number of seams.

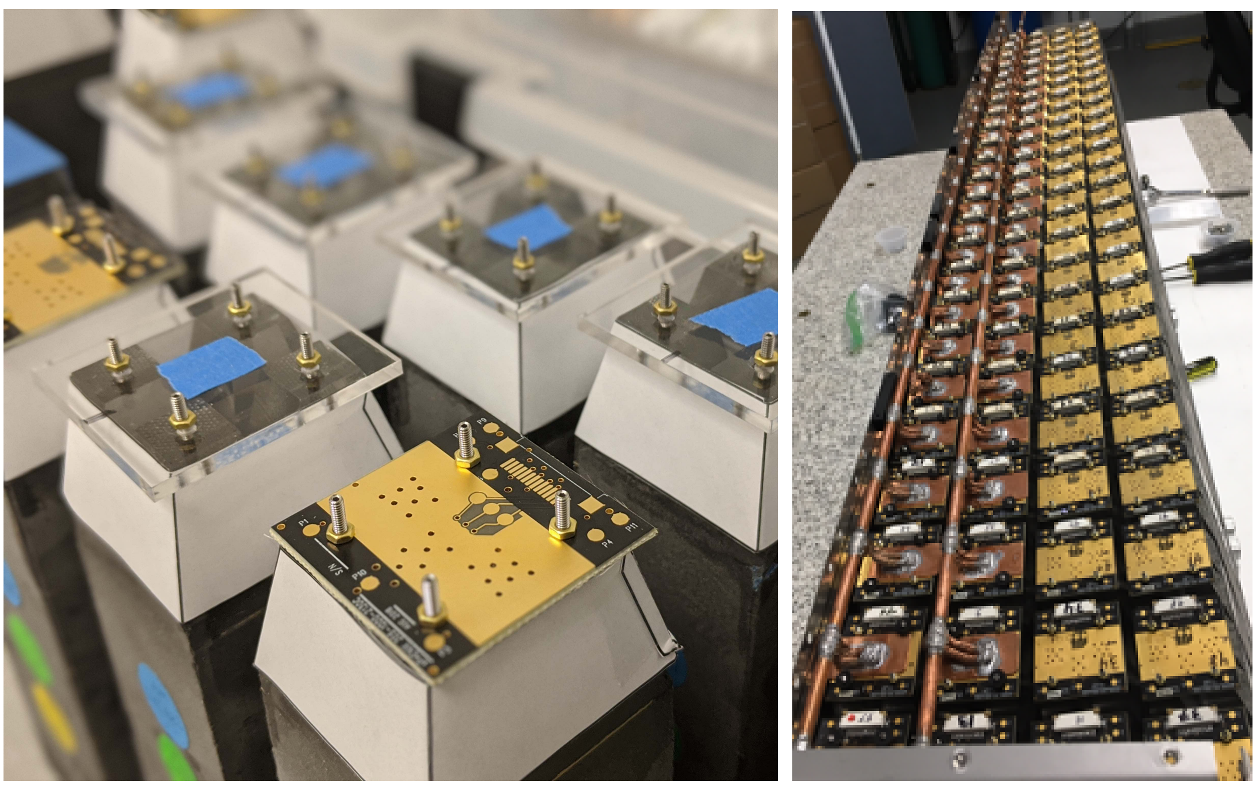

Figure 1.3: The EMCal blocks with light guides and readout mounting (left) and the assembled EMCal Sector "0" (right).

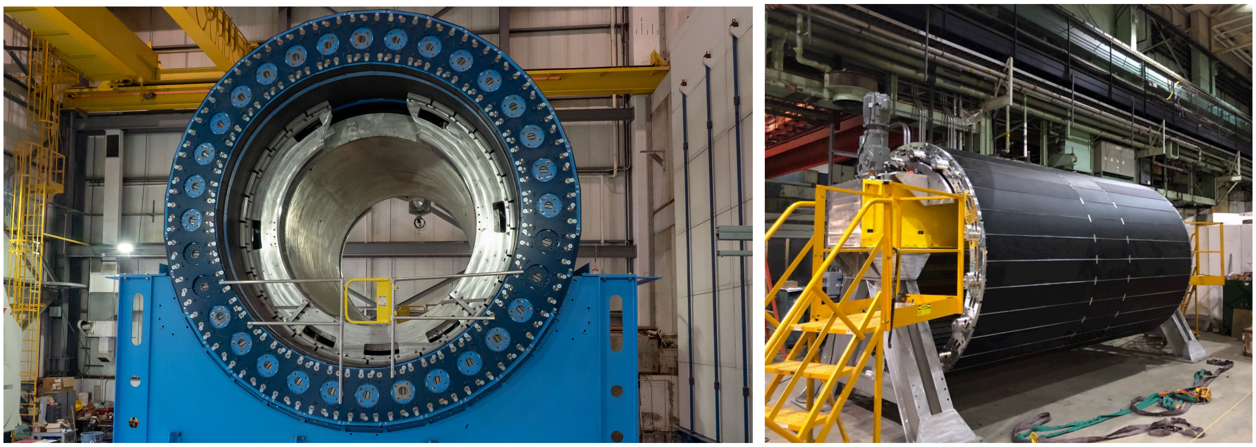

Figure 1.4: (left) All 32 sectors of the OHCal successfully installed in the experimental hall atop the carriage and around the sPHENIX magnet. (right) Assembled IHCal barrel at BNL. The iHCal is also an important support structure for all the detectors inside the bore of the Babar superconducting solenoid.

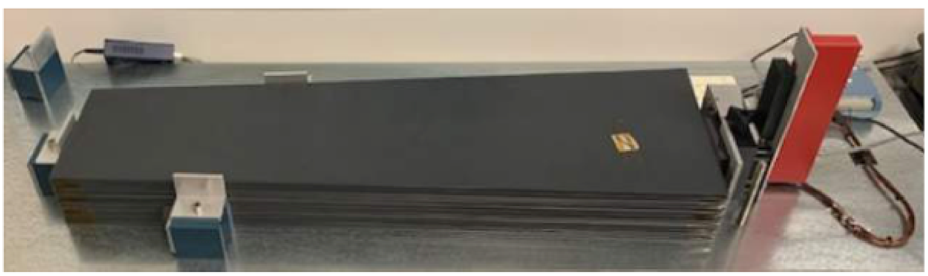

Figure 1.5: Testing the HCal scintillator tiles at GSU.

Figure 1.6: The minimum bias detector, originally built by Hiroshima University for PHENIX.

1.4.2 Infrastructure and Facility Upgrade

The Infrastructure and Facility Upgrade project consists of modifications to the 1008 facility needed to support the MIE and other detectors, most importantly support of the former BaBar solenoid into the RHIC cryogenic and power supply systems. The solenoid was tested at full field at BNL in

2018, and additional cryogenic equipment has been designed, reviewed, and purchased.

All the support systems for the detector, such as the power distribution and safety systems, and the integration and installation of the detector are designed and managed as part of this project. While the planned beam pipe was lost in a transit accident in early 2022, a replacement beam pipe from STAR is being modified for use in the interaction region.

1.4.3 Inner HCal

The support structure of the electromagnetic calorimeter has been instrumented with scintillating tiles similar to the tiles used in the Outer HCal as part of the Inner HCal project. All IHCal scintillating tiles have been delivered from the vendor and have been tested both at the vendor and at Georgia State University (GSU) upon receipt, as shown in Figure 1.5. They have now all been assembled into the IHCal barrel, and are ready for installation into the magnet bore, as seen in Figure 1.4 (right).

1.4.4 High-Rapidity EMCal

The section of the barrel EMCal with $|\eta| > 0.85$ was de-scoped before CD-1/3A, however it has been restored through collaboration with institutions in China. The large-rapidity tungsten/scintillating fiber blocks produced at Fudan University have been shipped to UIUC and have successfully passed examination and characterization tests, and are now assembled into the EMCal sectors.

1.4.5 MVTX

The detector nearest the collision point is the MVTX, a silicon pixel detector closely based on the ALICE ITS inner barrel using Monolithic Active Pixel Sensors (MAPS). Figure 1.7 shows the design of a half barrel, designed to clam-shell over the beam pipe. The MVTX is capable of 5 μm resolution for tracks with $p_T > 1$ GeV and enables the heavy-flavor tagged jet and open heavy-flavor programs. Production of the MVTX staves is underway at CERN, and a custom carbon fiber support structure has been designed at MIT and LANL with engineering assistance from LBNL. Two of the production MVTX staves are shown in Figure 1.8.

1.4.6 INTT

The INTT is a silicon strip detector surrounding the MVTX, with a rendering shown in Figure 1.9. This detector interpolates tracks between the extremely fine pitch of the MVTX and the coarser spatial resolution of the TPC. It is also the only tracking detector with single-beam-crossing timing resolution — the ability to uniquely associate hits with a specific bunch crossing — and is therefore key to associating fully reconstructed tracks with the event that produced them. The INTT is nearly finished with production and testing and will soon be ready for installation.

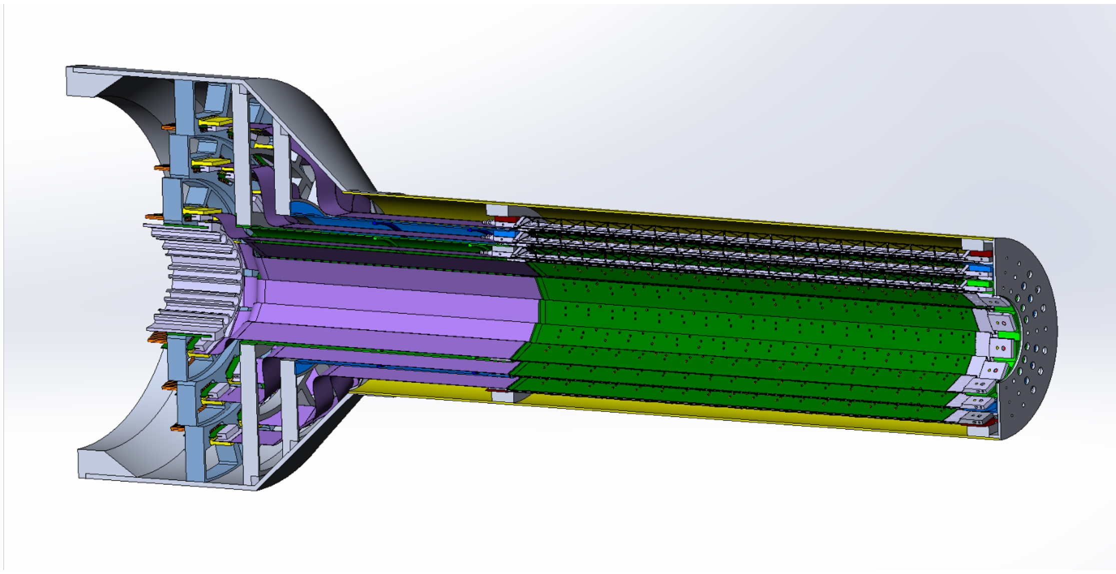

Figure 1.7: A rendering of a half barrel of the MVTX in its carbon fiber support structure.

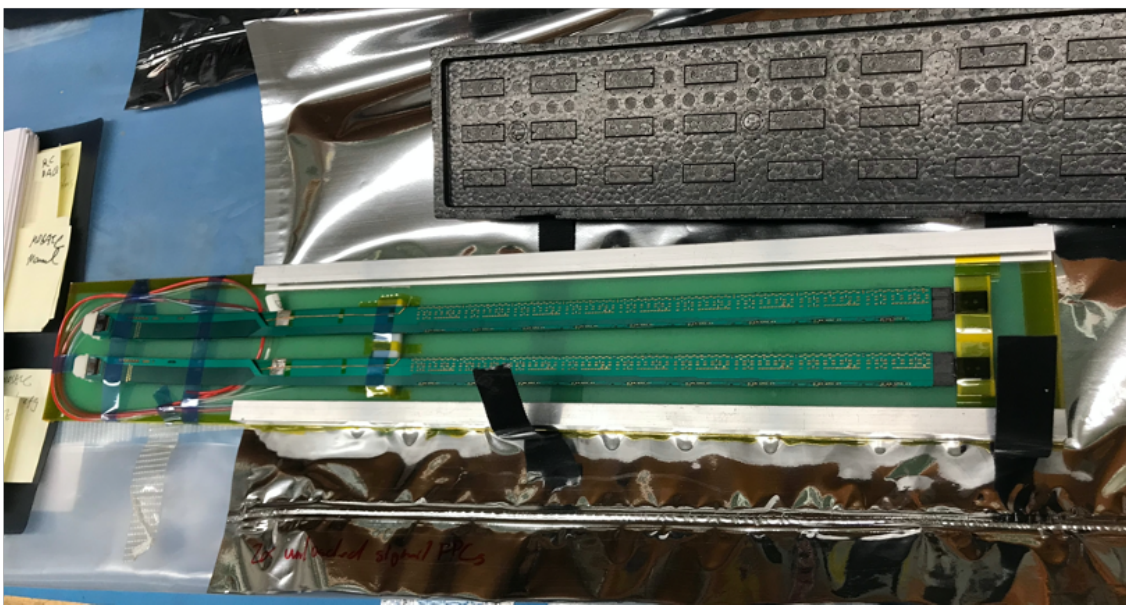

Figure 1.8: Two of the production MVTX staves. These are nearly identical to the ALICE ITS inner barrel staves. The only modification is the use of a slightly longer power cable soldered to the stave.

1.4.7 Event Plane Detector

The sPHENIX Event Plane Detector (sEPD) consists of two wheels of scintillator tiles positioned at $2 < |\eta| < 4.9$. The sEPD, similar to the existing STAR EPD, provides significantly improved event plane (EP) resolution compared to the MBD with a large rapidity gap between the EP determination and the mid-rapidity measurement region. The sEPD is funded by a NSF MRI grant with Lehigh, UNC Greensboro, CU Boulder, Muhlenburg, and BNL as participating institutions.

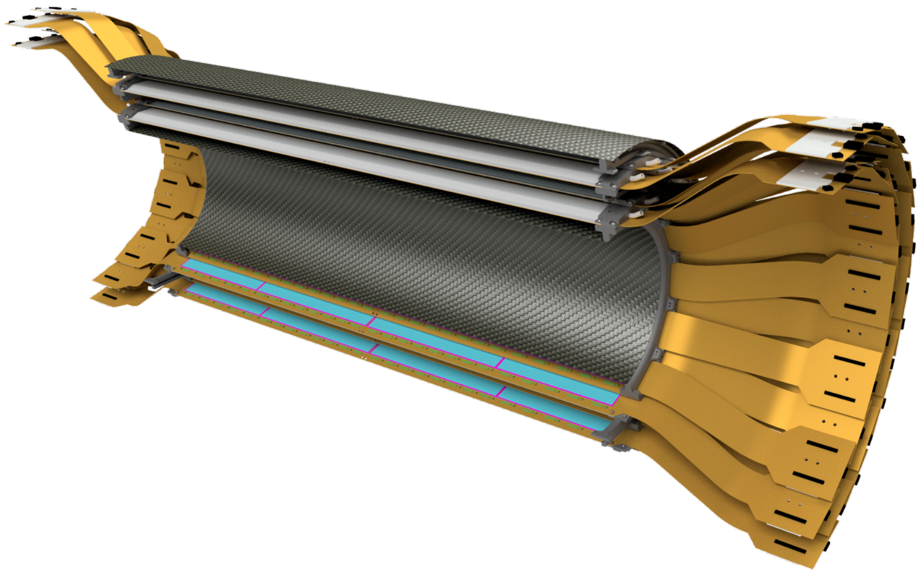

Figure 1.9: A rendering of the silicon strip intermediate tracker (INTT), being built by RIKEN and NCU Taiwan. While the sensors (blue) are off-the-shelf Hamamatsu parts, the flexible high density cables (orange) which carry signals and power have been a target of extensive R&D with industrial partners due to their length.

1.4.8 TPOT

The TPC Outer Tracker (TPOT) is a Micromegas-based tracker consisting of eight modules situated between the bottom side of the TPC and the EMCal. The TPOT will help monitor space-charge distortions in the TPC by providing an extra space point to improve track extrapolation accuracy from the MVTX and INTT into the TPC. TPOT is a collaborative effort between groups at CEA-Saclay, LANL, MIT and BNL.

Chapter 2

Beam Use Proposal 2023–2025

In this Chapter we detail the sPHENIX Beam Use Proposal as requested in the Associate Laboratory Director Charge for three years of running during the period 2023–2025 assuming 24 or 28 cryo-weeks in each year. The complete charge is reproduced in Appendix A.

2.1 Years 2023–2025 Proposal

The three-year proposal is summarized in Table 2.1. The numbers correspond to 24-cryo weeks in each year with alternate numbers in parenthesis corresponding to 28-cryo weeks. The recorded luminosity values correspond to events collected via minimum bias triggers that sample a large fraction of the inelastic cross section ($>$ 90% in Au+Au for example). These events have collision vertex $|z| < 10$ cm that corresponds to the optimal acceptance range for the full sPHENIX detector, including the inner tracker.

In 2024, we include two sets of values, with the first corresponding to simply recording 5 kHz of minimum bias data in p+p and p+Au collisions. The second value is with minor data acquisition upgrade for partial streaming readout (10%-*str*) for the Time Projection Chamber (TPC) and the inner tracking detectors (MVTX, INTT). Thus, these recorded luminosities are for the tracking detectors only, i.e. without the calorimeters. Details on the streaming readout upgrade are given in Chapter C. The sampled luminosity values correspond to additional events that are efficiently sampled with physics specific Level-1 triggers with trigger efficiencies greater than 90%. In this document we detail specifically which physics channels are enhanced from these Level-1 triggers.

The first year 2023 of running has significant commissioning time for the detector, and critically for the accelerator-detector combination, as expected for any new major, complex collider experiment. It is critical that this commissioning time be with Au+Au collisions at 200 GeV to insure a full understanding of the detector operation and performance under high occupancy conditions. Details on the commissioning plan are given in Chapter 3. After the commissioning period, 9 (13) weeks of physics data taking are available corresponding to recorded Au+Au minimum bias data sets of 25 (39) billion events. The main Au+Au physics run is in the third year, 2025, with more than 113 (141) billion events recorded in total for 2023 and 2025 running combined. Note that for all the luminosity projections and conversions to collision rates we utilize as total inelastic cross sections:

Table 2.1: Summary of sPHENIX Beam Use Proposal for the years 2023–2025, as requested in the charge. The values correspond to 24 cryo-week scenarios, while those in parentheses correspond to 28 cryo-week scenarios. The 10%-*str* values correspond to a streaming readout of the tracking detectors. Full details are provided in Chapter 2.

Year	Species	$\sqrt{s_{NN}}$ [GeV]	Cryo Weeks	Physics Weeks	Rec. Lum. $\|z\| <10$ cm	Samp. Lum. $\|z\| <10$ cm
2023	Au+Au	200	24 (28)	9 (13)	3.7 (5.7) nb^{-1}	4.5 (6.9) nb^{-1}
2024	$p^{\uparrow}p^{\uparrow}$	200	24 (28)	12 (16)	0.3 (0.4) pb^{-1} [5 kHz] 4.5 (6.2) pb^{-1} [10%-*str*]	45 (62) pb^{-1}
2024	$p^{\uparrow}$+Au	200	–	5	0.003 pb^{-1} [5 kHz] 0.01 pb^{-1} [10%-*str*]	0.11 pb^{-1}
2025	Au+Au	200	24 (28)	20.5 (24.5)	13 (15) nb^{-1}	21 (25) nb^{-1}

6.8 barns, 1.7 barns, 42 millibarns for Au+Au, p+Au, and p+p, respectively.

The second year, 2024, of running provides the critical baseline measurements in p+p and p+Au both at $\sqrt{s_{NN}} = 200$ GeV. The proton beam in both cases will be with transverse (vertical) polarization. These data sets provide key baseline measurements for nuclear modification factors R_{AA}, R_{pA}, new collectivity and probes of small collision systems, as well as compelling transverse spin physics observables. We highlight that particularly in this year, the 24 cryo-week scenario is challenging since new Level-1 triggers will be commissioned and C-AD requires a significant number of cryo-weeks for switching systems.

In the following sections, we detail the running conditions worked out with the Collider-Accelerator Division (C-AD) experts. We then provide detailed cryo-week breakdowns for each running year, along with explicit assumptions for calculating the recorded and sampled luminosities.

Specific details on the RHIC luminosity projections, mapping out of cryo-weeks schedules, and overall trigger/sampling calculations are given in the next Sections.

2.2 RHIC Luminosity Projections

For planning purposes, C-AD provides luminosity projections in a periodically updated document which utilizes knowledge gained from the Run-15 p+p and p+Au at 200 GeV running and the Run-16 Au+Au at 200 GeV running. The most recent version is available at: `http://www.rhichome.bnl.gov/RHIC/Runs/RhicProjections.pdf` .

From 2019 to early 2022, the versions of this document featured a stable set of projections which were used for the preparation of this Beam Use Proposal (in 2022) and two previous ones (2020 and 2021). In May 2022, shortly before the submission of this BUP, C-AD released updated guidance in which the Au+Au and p+Au projections were largely unchanged.

However, the new guidance suggests a moderate (up to 20%) potential reduction in the expected p+p luminosity in 2024 running. Given the short time frame, the projections in this BUP were not able to be updated to account for the decreased p+p baseline. A qualitative way to understand the impact would be increase the statistical uncertainty by 10% on all measurements which use the full sampled p+p luminosity (jets, photons, Upsilons). However, many measurements would also become increasingly sensitive to uncertainties where large statistics are needed to study systematic effects in data (e.g. isolated track-to-calorimeter matching for inter-detector energy calibration, γ+jet calibration of the energy scale in p+p) in a way that is difficult to quantify quickly.

We strongly stress the critical need for high-luminosity p+p reference data for the sPHENIX physics program. The p+p baseline is the dominant contributor to the statistical uncertainties in many of the unique, flagship sPHENIX measurements (such as Upsilon suppression). We note that a decreased luminosity has the same practical effect as a decreased running time, and highlight the importance of a full 28 cryo-week run in 2024 to allow for both p+p and p+Au running with sufficient statistics. If possible, sPHENIX is also prepared to run for a longer period in 2024 in order to collect the crucial p+p reference data.

Below, we describe the quantitative translation of the C-AD projections into expected event rates at sPHENIX for 2023-2025. In the planning document, C-AD provides a minimum and maximum luminosity per week for each running period, as well as the fraction of collisions within a given z-vertex range. For calculating the integrated luminosity, we assume a ramp-up curve and then a steady-state physics running at the mean of the minimum and maximum in both luminosity and z-vertex fraction within $|z| < 10$ cm (where a minimum and maximum are given). We also highlight that a critical part of the sPHENIX run plan is to have a non-zero crossing angle between the beams – the crossing angle reasoning, implications, and quantitative analysis in Chapter B. Finally, in the preparation of projections for polarized observables, we use the expected polarization given by the C-AD guidance, i.e., under the assumption that any present issues with the Blue ring Siberian snake are resolved prior to 2024 running.

We assume an sPHENIX up-time (i.e. the fraction of time when collisions are available when sPHENIX is taking data with high livetime) of 0.60 for the first two years of running (2023 and 2024) since the detector is being commissioned for new collision systems and new Level-1 triggers are being brought online, and 0.80 for subsequent running (2025). These up-time values fold in the expected deadtime of the data acquisition system, which is greater than 90%.

RHIC C-AD projections for time in store (i.e. RHIC up-time) vary slightly with most of the projected values around 0.60. It is notable that C-AD projections are for a nominal 8 hour store; however, a more optimal store length may be found in future running at closer to 5 hours.

Weeks	Designation
0.5	Cool Down from 50 K to 4 K
2.0	Set-up mode 1 (Au+Au at 200 GeV)
0.5	Ramp-up mode 1 (8 h/night for experiments)
11.5	sPHENIX Initial Commission Time
9.0 (13.0)	Au+Au Data taking (Physics)
0.5	Controlled refrigeration turn-off
24.0 (28.0)	Total cryo-weeks

Table 2.2: Year 2023 run plan for 24 (28) cryo-weeks with Au+Au 200 GeV collisions.

2.3 Cryo-Weeks

For mapping out a run plan, we state both cryo-weeks for a running period and also physics data taking weeks, i.e. when Physics Running is declared by C-AD. The guidance from C-AD is that there is a 0.5 week "cool down from 50 K to 4 K", then a 2.0 week "set-up mode" for the specific collision species, and then a 0.5 week "ramp-up". If switching species, there is again a 2.0 week "set-up" and 0.5 week "ramp-up". Lastly, at the end of the running period, there is a 0.5 "warm-up from 4 K to 50 K". In addition, we assume that in the first, second and third weeks of declared Physics Running, one achieves 25%, 50%, and then 75% of the luminosity target, with subsequent weeks at 100%. These are standard assumptions following C-AD guidance.

Following said C-AD guidance, we present the cryo-week break downs for the 24 (28) week scenarios. These are shown for each year (2023-2024) in Tables 2.2, 2.3, and 2.4, respectively.

2.4 Sampled versus Recorded Luminosity

In the Au+Au 200 GeV case, the physics will predominately come from **recorded** minimum bias collisions. This data will be selected by the Level-1 trigger via the MBD that samples approximately 90% of the inelastic cross section. Additional physics may be "sampled" with rare event triggers, for example high-p_T direct photons, where the trigger rejection is very high even in central Au+Au events. All physics projections are based on the recorded luminosity in Au+Au unless otherwise stated. The key requirements to achieve these recorded event sets are (1) the sPHENIX Data Acquisition Level-1 accept rate of 15 kHz with livetime greater than 90%, (2) the luminosity corresponds to a rate of collisions within $|z| < 10$ cm during the store above 15 kHz, and (3) maintaining the sPHENIX and RHIC uptime projections. As shown in Figure 2.1, the projected Au+Au collision rate within $|z| < 10$ cm exceeds the 15 kHz minimum bias recording capacity for

Weeks	Designation
0.5	Cool Down from 50 K to 4 K
2.0	Set-up mode 1 ($p^{\uparrow}p^{\uparrow}$ at 200 GeV)
0.5	Ramp-up mode 1 (8 h/night for experiments)
12.0 (16.0)	Data taking mode 1 ($p^{\uparrow}p^{\uparrow}$ Physics)
1.0	Move DX magnets
2.0	Set-up mode 2 ($p^{\uparrow}$+Au at 200 GeV)
0.5	Ramp-up mode 2 (8 h/night for experiments)
5.0	Data taking mode 2 ($p^{\uparrow}$+Au Physics)
0.5	Controlled refrigeration turn-off
24.0 (28.0)	Total cryo-weeks

Table 2.3: Year 2024 run plan for 24 (28) cryo-weeks with $p^{\uparrow}p^{\uparrow}$ and $p^{\uparrow}$+Au 200 GeV collisions.

Weeks	Designation
0.5	Cool Down from 50 K to 4 K
2.0	Set-up mode 1 (Au+Au at 200 GeV)
0.5	Ramp-up mode 1 (8 h/night for experiments)
20.5 (24.5)	Au+Au Data taking (Physics)
0.5	Controlled refrigeration turn-off
24.0 (28.0)	Total cryo-weeks

Table 2.4: Year 2025 run plan for 24 (28) cryo-weeks with Au+Au 200 GeV collisions.

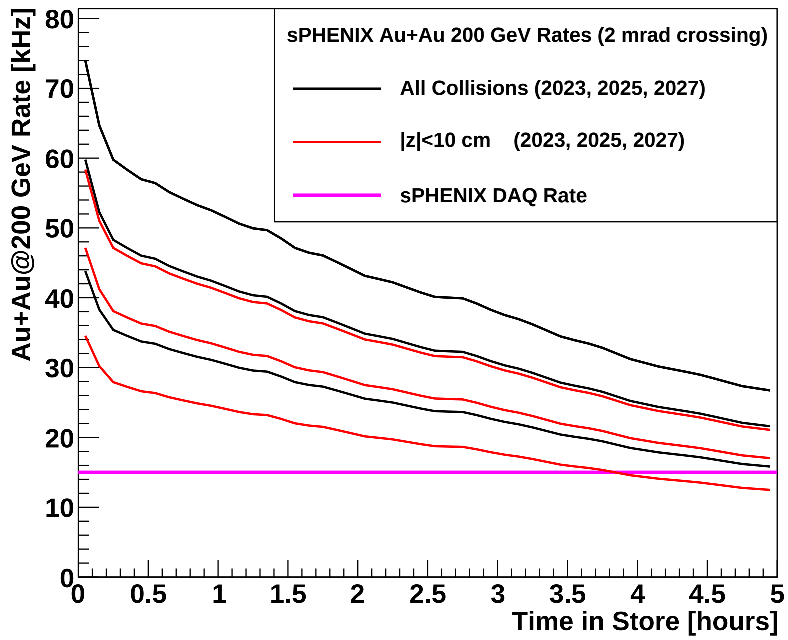

Figure 2.1: Estimated Au+Au at 200 GeV collision rate as a function of Time in Store for all collisions (black) and collisions within ± 10 cm (red). The bottom to top set of curves in each color are for the mean luminosity and fraction within ± 10 cm for the C-AD projections labeled in their document as 2023, 2025, 2027, with the maximum projections for 2025 and 2027. Also shown as a magenta line is the sPHENIX Data Acquisition Level-1 accept rate of 15 kHz for reference.

most of a five-hour store. Thus a factor of ≈ 1.5, depending on the year, that can be additionally sampled by very selective physics triggers in Au+Au even at the lower luminosity selection.

In the p+p and p+Au case, the physics will predominantly come from **sampled** Level-1 triggered events utilizing photon, electron (e.g. from Upsilon decays), hadron, and jet triggers. Thus, the key value is the sampled luminosity for these physics channels. Note that some observables such as lower p_T hadrons (and in particular heavy-flavor hadrons D, Λ_c, B) do not have effective Level-1 physics triggers. Thus, in these cases the recorded luminosity is crucial. We have nominally allocated 5 kHz, out of the 15 kHz Level-1 trigger rate, for p+p and p+Au minimum bias collection. A critical addition is the streaming capability for the tracking detectors, which enables much larger minimum bias data sets (without calorimeter readout).

Trigger algorithms have been developed and tested for p+p and p+Au running using the EMCal for single photons (typically with p_T greater than 10 GeV) and for electrons (from Upsilon decays typically with p_T greater than 3–4 GeV). In addition, trigger algorithms using the combined EMCal and HCal information have been developed for selecting jets and single hadrons. At the highest p+p interaction rates, rejection factors of order 5000–10,000 are needed to result in a 1–2 kHz bandwidth allocation for a given trigger channel. Full GEANT-4 simulations with HIJING p+p and p+Au events have been used to document the trigger efficiencies and rejection factors for all Level-1 algorithms. One example set of calculations for jet triggers is shown in Figure 2.2 indicating good efficiency and rejection factors above the required level.

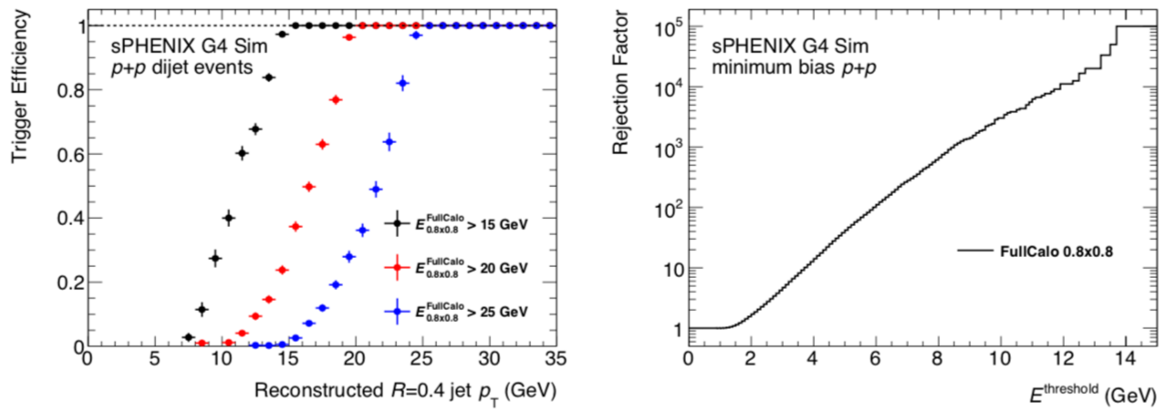

Figure 2.2: sPHENIX full GEANT-4 simulations with HIJING $p+p$ events run through the jet Level-1 trigger emulator with efficiencies (left) and rejection factors (right).

Species	Year 1–3 Total	$\langle N_{coll} \rangle$	Effective-$p+p$
$p+p$	62 pb^{-1} (sampled)	1	2.4×10^{12}
$p+$Au	0.11 pb^{-1} (sampled)	4.7	0.9×10^{12}
Au+Au	20.7 nb^{-1} (recorded)	250	35×10^{12}

Table 2.5: Comparison from the full data sets from Years 2023–2025 assuming the 28 cryo-week scenarios for the three systems $p+p$, $p+$Au, Au+Au.

Table 2.5 details the number of relevant events recorded or sampled for measuring high p_T jets from running in 2023–2025. For Au+Au minimum bias events, the average number of binary collisions is $\langle N_{coll} \rangle \approx 250$. Similarly, for $p+$Au the $\langle N_{coll} \rangle = 4.7$. We note that the Au+Au sample with an order of magnitude more effective $p+p$ collisions sampled will be divided into multiple centrality bins and jet quenching will reduce the statistics at high p_T. This is a reasonable balance of cold and hot system measurements.

Chapter 3

sPHENIX Commissioning

Significant commissioning time is required to prepare for physics quality data later in the first run. The sPHENIX project and collaboration teams have taken this task seriously with detailed input from the detector subsystems and the sPHENIX Physics Working Groups. The collaboration has created a Commissioning Task Force comprised of member of sPHENIX project management and knowledgeable scientists and engineers from all detector systems including the core MIE detectors as well as the MVTX, INTT, IHCAL, sEPD, and TPOT detectors, electrical and electronic infrastructure, and online software and computing.

Every running period with a new collision species requires specific commissioning, particularly in terms of safely bringing the beams to full intensity, setting up the beam crossing angle, timing in the detectors, and setting up the Level-1 triggers. However, the very first running of the detector in 2023 requires significant additional commissioning time for each subsystem and for confirming full detector performance specifications are being met. Therefore we provide a dedicated week-by-week plan for detector commissioning in the 2023 Au+Au run in Section 3.1. Commissioning in the 2024 $p+p$ and $p+$Au running is built into the ramp up during physics data taking weeks.

3.1 2023 Au+Au Commissioning Timeline

Commissioning sPHENIX with beams in RHIC should progress in stages with gradually increasing luminosity. Au+Au collisions are necessary for commissioning of the detector under high multiplicities conditions. We note that installation of the sPHENIX inner silicon detectors takes 2–3 weeks and thus these sensitive detectors will be installed ahead of the 2023 running period. The presence of the full detector configuration means that very careful monitoring of luminosity and beam conditions is essential to maintain stable operations and minimize detector risk. Thus, the sPHENIX experiment will require very careful coordination with C-AD including potential accelerator down times for access. A summary of the projected initial commissioning timeline is shown in Table 3.1.

For the purposes of this Beam Use Proposal, we include a very brief summary of considerations behind the timeline as given. Except for initial stores with fewer bunches, operation with the maximum number of bunches (111) is preferable to reducing luminosity by reducing the number

Weeks	Details
2.0	low rate, 6-28 bunches
2.0	low rate, 111 bunches, MBD L1 timing
1.0	low rate, crossing angle checks
1.0	low rate, calorimeter timing
4.0	medium rate, TPC timing, optimization
2.0	full rate, system test, DAQ throughput
12.0	**total**

Table 3.1: Timeline for sPHENIX commissioning period in 2023, the first year of operation.

of filled bunches, because it allows sPHENIX to commission as it plans to run. Initial stores should be at zero crossing angle, both to begin operations with stores less likely to be lost as well as to provide a direct comparison of vertex distribution between crossing angles of zero and the nominal 2 milliradians.

The superconducting solenoid should be operating at full field during the commissioning. The minimum bias detector (MBD) gains are reduced by the magnetic field, and so tuning should take place at the field planned for physics operation.

- Initial studies will require two weeks of stores with 6 to 28 bunches, zero crossing angle, and a collision rate of up to 2 kHz. These collisions will be used for an initial tune-up of timing and the MBD trigger. A simple ”blue logic” trigger, i.e. with standard NIM modules, may be used initially for timing. Several days will be required before we can fully operate the detector and time is needed for diagnostic instrumentation and processing of data. During this period the stores can be kept in RHIC as long as is practical.
- The next period will consist of two weeks of stores with 111 bunches, zero crossing angle, and a collision rate of 1–5 kHz. These stores will be used for optimizing the MBD Level-1 (L1) trigger, which may require additional timing adjustments of the trigger primitives. This phase will also require relatively short periods of data taking followed by analysis and diagnostics. Near the end of this period, the calorimeters could be turned on, and timing them in could be attempted if it was not already done during the previous period. Operation during the second week will employ the planned crossing angle. This should allow the first measurement of the vertex distribution with the planned crossing angle and begin any optimization of the ramp that may be necessary while the tracking detectors, including the two inner silicon detectors, are turned off.
- We estimate that it will take a week of machine studies at this point to optimize the beam crossing angle. Careful coordination between sPHENIX and RHIC operations will be important in

this stage.

- The next week will consist of stores with 111 bunches and non-zero crossing angle, and will be used for calorimeter timing and tuneup. The crossing angle will allow us to assess the radiation dosage to the silicon photo-multipliers (SiPMs) by measuring the leakage current with the monitoring system.
- The next phase will consist of four weeks of stores with 111 bunches, non-zero crossing angle, and a collision rate of 1–5 kHz. These stores will be used for initial operation of the tracking detectors, beginning with the TPC. The minimum bias trigger, developed in the previous weeks, will be used to trigger the detector readout. It may be useful during this phase to operate with zero magnetic field and/or very low luminosity for periods of time in order to collect data which can be used to align the tracking detectors and characterize track distortions. Some additional time may be necessary for data taking at zero field in order to change the MBD high voltage for zero field.
- The next two weeks will involve stores with 111 bunches, non-zero crossing angle, and an increasing rate of minimum bias collisions, culminating in fills that provide 15–20 kHz of collisions in order to stress test the data acquisition system under target running conditions.

At the end of this 12 week commissioning plan, the detector should be ready to take data with all sub-systems, triggered according to plan for Au+Au, at the design rate of the data acquisition system. Of course, producing data of publication quality requires more analysis than can be brought to bear while the collaboration is commissioning the apparatus, so it is crucial to develop monitoring software which allows us to quickly assess the quality of data as we take it. We note that such commissioning time always has a significant uncertainty, and run time flexibility in this first year will be required.

Additional trigger specific commissioning time is needed for each new collision species, particularly the physics-selective Level-1 triggers in the 2024 $p+p$ and $p+$Au running. This commissioning time is built into the ramp up calculation for integrated luminosities in these periods. For projections, we have estimated 60% up-time for the sPHENIX detector in 2023 and 2024 during physics running, and then an 80% up-time in 2025.

3.2 New considerations for 2023 Au+Au Commissioning

The first run of a largely new experiment at RHIC will require the development of many new operational procedures, and flexibility in operating RHIC and the experiment. Some specific differences are:

- The calorimeters are read out with silicon photomultipliers which are sensitive to radiation damage by slow neutrons. Estimates have been made of the expected radiation dose have been made based on measurements at STAR and PHENIX and with Monte Carlo, but it is important to minimize the dose delivered to the calorimeters.
- The detector will be operated from the beginning with silicon detectors close to the beam pipe which can potentially be damaged by catastrophic beam loss. For this reason, spurious

abort kicker prefires may be particularly serious and all possible measures should be made to avoid them during sPHENIX operation.

- Access to the detector may be necessary more frequently during the commissioning period than has been customary with more mature detectors, and access more frequently than weekly access will be necessary and should be a priority in initial operation.

- Initial commissioning will include the development of data to be transmitted to Main Control which will allow monitoring sPHENIX operation, but initially, only rudimentary monitoring may be available.

Chapter 4

Physics Projections 2023–2025

In this Chapter we present some of the key physics that sPHENIX will deliver with the run plan for 2023–2025 that was detailed in Chapter 2. The projected uncertainties shown in the following sections have been determined for the 28 cryo-week scenarios. It is straightforward to rescale the uncertainties to obtain projections for 24 cryo-week scenarios. In the case of nuclear modification factors, the results include uncertainties in the numerator from the Au+Au or p+Au running and the denominator from the p+p reference data sets. The physics projections are split into Section 4.1 (Jet and Photon Physics), Section 4.2 (Upsilon Physics), Section 4.3 (Open Heavy Flavor Physics), and Section 4.4 (Cold QCD Physics).

4.1 Jet and Photon Physics

Probing the quark-gluon plasma with precise jet, direct photon, and hadron measurements is a core component of the sPHENIX scientific program. Between 2023 and 2025, sPHENIX will collect large data samples to allow for detailed reconstructed jet measurements, including jet yields, di-jet events, jet (sub-)structure and properties, photon-tagged jet quenching measurements, and jet-hadron correlations. The projections in this Section are for light flavor jets; projections for b-quark jet yields and their properties are discussed in Section 4.3.

The projections in this section are based on perturbative QCD calculations previously used in the sPHENIX MIE proposal document [5] applied to the nominal running plan proposed in Section 2. For p+p collisions, it is has been demonstrated that essentially all photons and jets can be efficiently selected, above a moderate p_{T} value ($\approx$ 20 GeV), by a calorimeter trigger and that the full high-p_{T} charged hadrons yield can be selected indirectly via a jet trigger. For Au+Au collisions, it is assumed that jets and charged hadrons will only be measured in minimum bias events, but that all high-p_{T} photons can be recorded by a dedicated photon trigger in Au+Au data-taking.

Figure 4.1 (left) shows the projected total yield of jets, direct photons, and hadrons in p+p collisions and in 0–10% central Au+Au collisions, using a Glauber MC simulation [6] to translate Au+Au event yields to an effective partonic luminosity. Overall suppression factors of $R_{\mathrm{AA}} = 0.2$, 0.4 and 1.0 are assumed for hadrons, jets, and photons in central Au+Au events. In the first three years, sPHENIX will have kinematic reach out to ~ 70 GeV for jets, and ~ 50 GeV for hadrons and

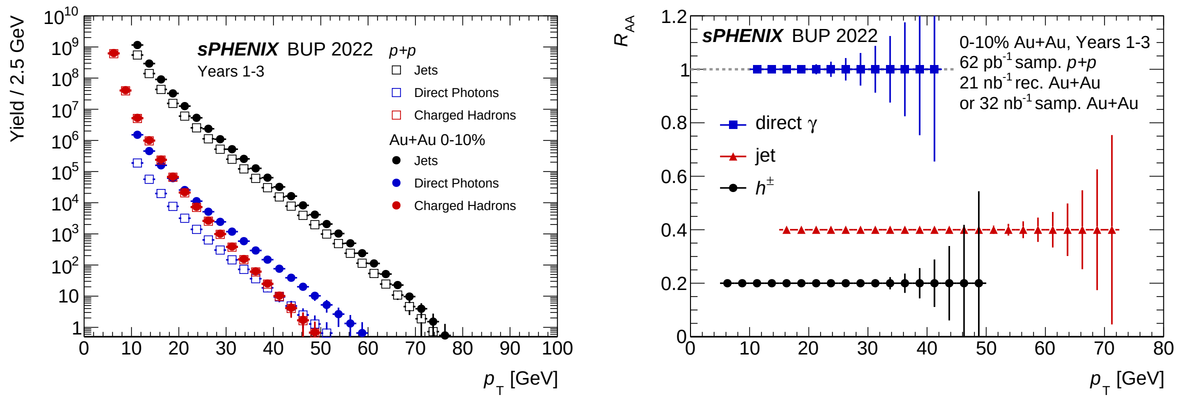

Figure 4.1: Projected total yields (left) and R_{AA} (right) for jets, photons, and charged hadrons in 0–10% Au+Au events and p+p events, for the first three years of sPHENIX data-taking.

Signal	Au+Au 0–10% Counts	p+p Counts
Jets $p_{\mathrm{T}} > 20$ GeV	22 000 000	11 000 000
Jets $p_{\mathrm{T}} > 40$ GeV	65 000	31 000
Direct Photons $p_{\mathrm{T}} > 20$ GeV	47 000	5 800
Direct Photons $p_{\mathrm{T}} > 30$ GeV	2 400	290
Charged Hadrons $p_{\mathrm{T}} > 25$ GeV	4 300	4 100

Table 4.1: Projected counts for jet, direct photon, and charged hadron events above the indicated threshold p_{T} from the sPHENIX proposed 2023–2025 data taking.

photons.

As another way of indicating the kinematic reach of these probes, the nuclear modification factor R_{AA} for each is shown in Figure 4.1 (right). There are varying theoretical predictions concerning the behavior of the R_{AA} at higher p_{T} which will be definitively resolved with sPHENIX data.

The projection plots above indicate the total kinematic reach for certain measurements, such as those which explore the kinematic dependence of energy loss. For other measurements, it is useful to have a large sample of physics objects to study the properties of their intra-event correlations, for example for jets (their internal structure), photons (for photon+jet correlations), and hadrons (for hadron-triggered semi-inclusive jet measurements). We illustrate the total yields in sPHENIX above some example p_{T} thresholds in Table 4.1.

Several specific examples of sPHENIX projections for jet correlations and jet properties follow below.

Figure 4.2 shows a statistical projection of the photon–jet p_{T} balance distribution, and of the sub-jet splitting function z_g, both in p+p events compared to that predicted by the JEWEL Monte Carlo

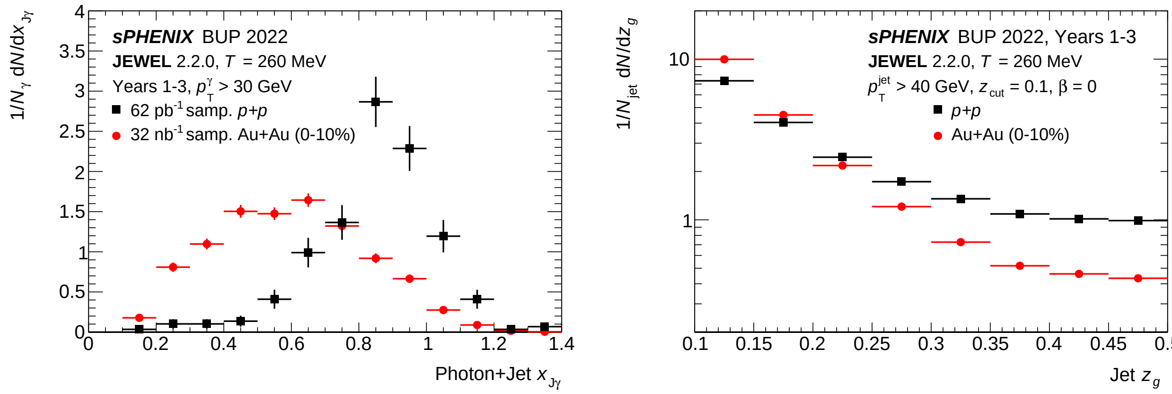

Figure 4.2: Statistical projections for (left) the jet-to-photon p_T balance, $x_{J\gamma}$, for photons with $p_T >$ 30 GeV and (right) the subjet splitting fraction z_g for jets with $p_T > 40$ GeV. Statistical uncertainties in the right panel are smaller than the markers. The projected distributions are sampled from those predicted according to JEWEL v2.2.0.

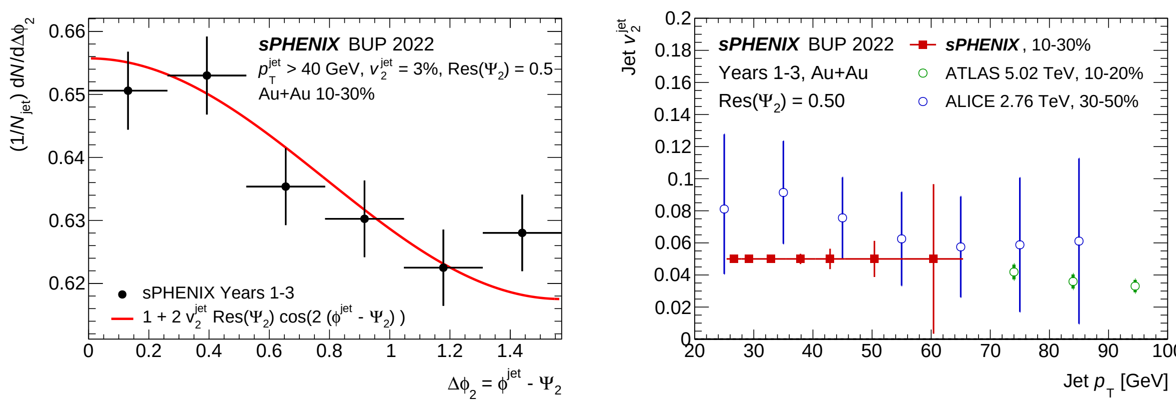

Figure 4.3: Left: Statistical projections for the jet yield as a function of the azimuthal distance from the event plane in 10–30% Au+Au events. Right: Statistical projection for a measurement of the jet v_2 in 10–30% events as a function of jet p_T, compared to that from ATLAS and ALICE at the LHC (where the error bars show the total statistical and systematic uncertainties together).

event generator [7] configured for RHIC conditions in 0–10% Au+Au central events. In both cases, sPHENIX will have large-statistics data samples to measure these specific distributions and investigate the associated physics.

Figure 4.3 which shows a statistical projection for a jet v_2 measurement in 10–30% Au+Au events. The azimuthal dependence of jet quenching is of particular interest since most theoretical calculations have been unable to simultaneously describe suppression and anisotropy at RHIC. The right panel compares the expected kinematic reach with measurements at the LHC by ATLAS [8] and ALICE [9]. Whereas the LHC can achieve a controlled measurement at high p_T, the systematic uncertainties grow substantially at lower p_T. sPHENIX is expected to have a significant advantage in measuring jets down to lower p_T given the lower RHIC energy, and the projection in Fig. 4.3 demonstrates that sPHENIX will have the required luminosity to constrain the jet v_2 in the range 25–60 GeV.

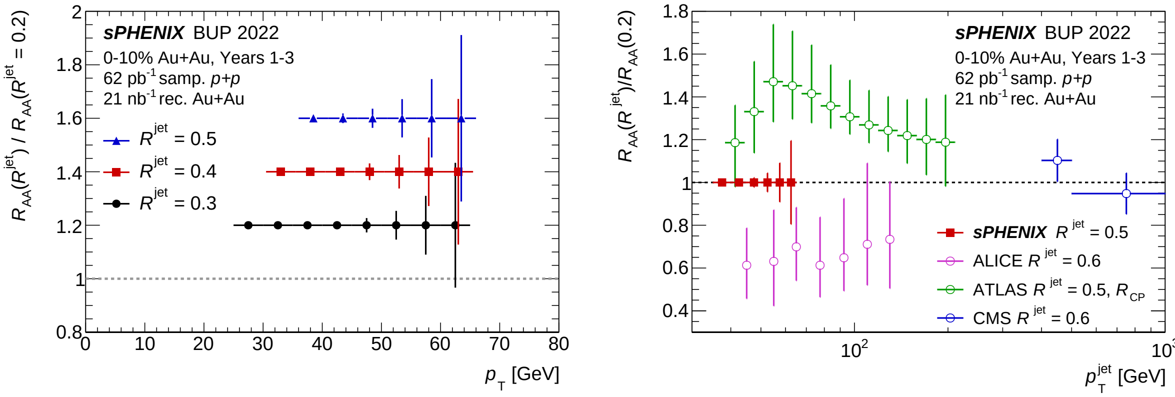

Figure 4.4: Left: Statistical projections for the jet R_{AA} double ratio between a large cone size and that for $R = 0.2$ in 0–10% Au+Au events. Right: Statistical projection for the R_{AA} double ratio for $R = 0.5$ compared to the latest similar measurements at the LHC.

Figure 4.4 shows a projection for suppression measurements of large-R jets in sPHENIX. These measurements probe the interplay of out-of-cone energy loss and the angular distribution of medium response effects, most recently highlighted by CMS [10]. For the projection in Figure 4.4, we expect that the jet R_{AA} for different jet R values can be reported in the kinematic region where the jet energy resolution is below 30%. Even with this conservative assumption, sPHENIX will be able to report the R-dependence of the R_{AA} over a wide p_{T} range and multiple cone sizes. The right panel compares the expected R_{AA} double ratio to the state of the art at the LHC. Note that in the low p_{T} region, the LHC experiments are in significant tension, with measurements featuring large, model-dependent uncertainties. sPHENIX can make a well-controlled measurement directly in this region of interest.

4.2 Upsilon Physics

High precision measurements of Upsilon production with sufficient accuracy for clear separation of the Υ(1S, 2S, 3S) states is a key deliverable of the sPHENIX physics program. The centrality dependence and particularly the p_{T} dependence are critical measurements for comparison between RHIC and the LHC, since the temperature profiles from hydrodynamic calculations show important differences with collision energy.

The projected statistical uncertainties for the R_{AA} of all three Υ states, including the Υ(3S), are shown in Figure 4.5 (left) as a function of the number of participants in the Au+Au collision. For the Υ(3S) projection, we assume that the R_{AA} for the Υ(3S) is approximately half of that for the Υ(2S), as observed in a recent measurement by CMS at the LHC. Thus, if the relationship between the 2S and 3S is reasonably similar at RHIC, sPHENIX has the opportunity to explore the systematics of the 3S suppression in some detail.

Figure 4.5 (right) shows the projected R_{AA} in 0–60% Au+Au events, as a function of Upsilon transverse momentum. For comparison, the latest STAR measurement of the 2S+3S together is shown. We highlight that the sPHENIX program offers the unique possibility to observe the strongly-suppressed $\Upsilon(3S)$ state at RHIC energies.

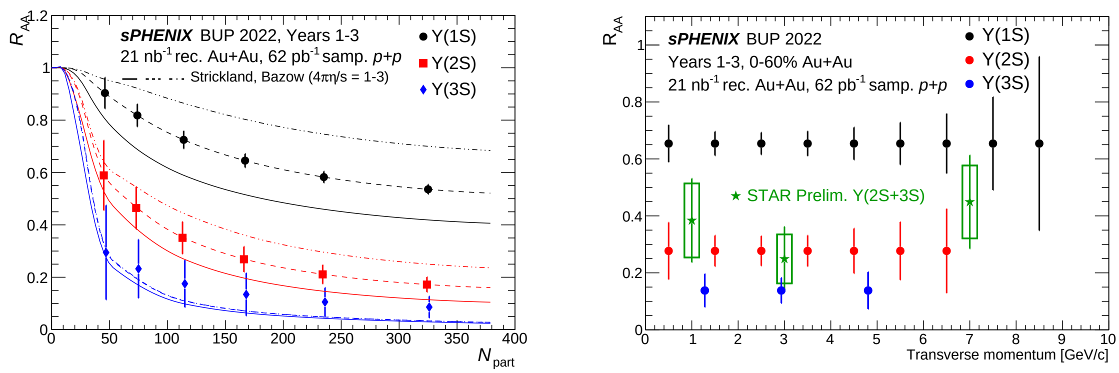

Figure 4.5: sPHENIX projected statistical uncertainties, including the contribution from uncorrelated backgrounds and physics backgrounds (such as from Drell-Yan and $b\bar{b}$), for the Upsilon nuclear modification factors for all three states. Projections for the proposed three-year (2023–2025) run plan are shown as a function of centrality (left) and p_T in 0–60% Au+Au events (right). In the left panel, the R_{AA} for the 1S and 2S is set to the prediction in Ref. [11], while the R_{AA} for the 3S is taken to be half that for the 2S. The right panel includes a comparison to the current best Upsilon suppression knowledge from STAR.

The centrality dependence and particularly the p_{T} dependence for all three states are critical measurements for comparison between RHIC and the LHC. Scenarios of melting of the different states at different temperatures must be confronted with data where the temperature profiles from hydrodynamic calculations show important differences with collision energy.

4.3 Open Heavy Flavor Physics

Heavy-flavor quarks (c, b) play a unique role in studying QCD in the vacuum as well as in the nuclear medium at finite temperature . Their masses are much larger than the QCD scale (Λ_{QCD}), the additional QCD masses due to chiral symmetry breaking, and the typical medium temperature created at RHIC and LHC ($T \sim 300$–500 MeV). Therefore, they are created predominantly from initial hard scatterings and their production rates are calculable in perturbative QCD. In combination with light sector measurements as discussed in Section 4.1, the large heavy quark mass scale introduces additional experimental and theoretical handles allowing one to study quark-QGP interactions in more detail and to better test our understanding of the underlying physics, including mass-dependent energy loss and collectivity in the quark-gluon plasma. Thus they can be used to study the plasma in a more controlled manner. However, heavy-flavor signals in heavy ion collisions at RHIC energies are relatively rare and current results from RHIC are sparse, particularly in the bottom sector. Improving on these results requires the sPHENIX capabilities of high precision and high data rate.

sPHENIX, equipped with a state-of-the-art vertex tracker and high rate streaming DAQ, will bring key heavy-flavor measurements at RHIC fully into the precision era and place stringent tests on models describing the coupling between heavy quarks and the medium. In the first three years of operation, sPHENIX will enable B-meson and b-jet measurements covering the wide transverse momentum range $2 < p_{\mathrm{T}} < 40$ GeV, as shown in Figures 4.6 and 4.7.

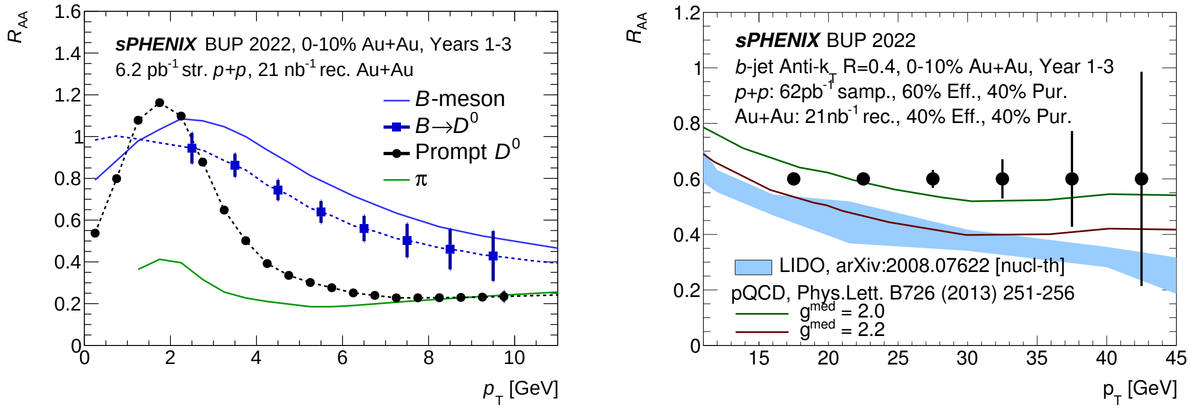

Figure 4.6: Projected statistical uncertainties of nuclear modification factor R_{AA} measurements of non-prompt/prompt D^0 mesons (left) and b-jets (right) as a function of p_T in 0–10% central Au+Au collisions at $\sqrt{s_{NN}} = 200$ GeV from the three-year sPHENIX operation. Left: the solid green curve are averaged R_{AA} for pions and the solid blue line is from a model calculation of R_{AA} for B mesons over several models [12, 13, 14, 15], which maps to the dashed blue line for D-meson from B decay. Right: the curves represents a pQCD calculations with two coupling parameters to the QGP medium, g^{med} [16], and the blue band is from a recent calculation based on the LIDO transport model [17].

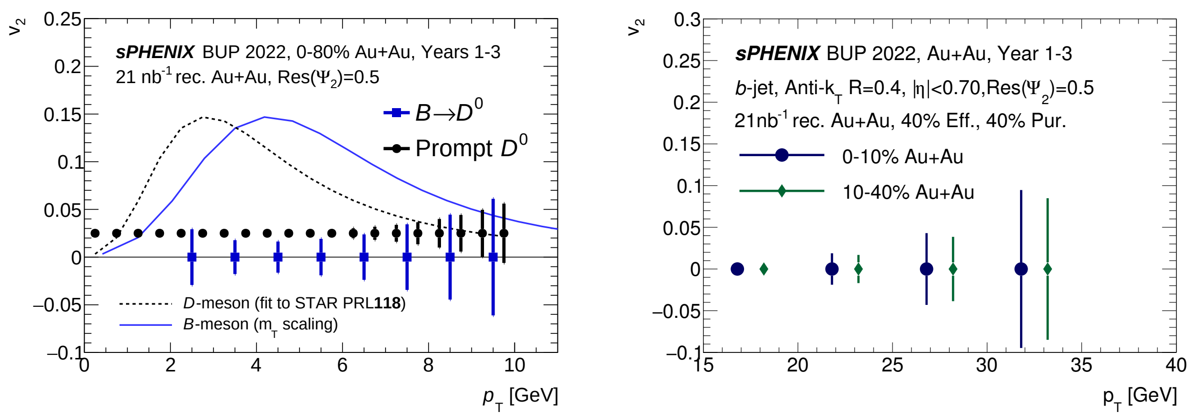

Figure 4.7: Projected statistical uncertainties of v_2 measurements of non-prompt/prompt D^0 mesons (left) and b-jets (right) as a function of p_T in Au+Au collisions at $\sqrt{s_{NN}} = 200$ GeV. Left: the blue dotted line is from best fit of RHIC data, and the black line is for B-meson assuming m_T scaling in v_2. [18, 12, 13, 14]

The left panel of Figure 4.6 shows the B-meson (D^0 from B) nuclear modification measurements covering the kinematic range $p_T \lesssim 15$ GeV, where nuclear modifications for bottom quarks and light quarks are expected to be quite different, transitioning in the right panel to the b-jet at $p_T > 15$ GeV, where the effect due to the light and heavy quark mass difference is less significant. The current experimental results do not yet confirm the detailed physics behind this transition.

Figure 4.7 (left) shows the elliptic flow v_2 measurements of the charm and bottom meson made with unprecedented precision that offer unique insight into the coupling of the HF quark to the medium. Theoretical modeling using the "Brownian" motion methodology requires that momentum transfer for each interaction is much smaller than the heavy particle mass [19]. It is thus much better controlled for bottom quarks compared to charm quarks [20]. Therefore, precision bottom measurements over a wide momentum range, particularly in the low-p_T region, can offer significant constraints on the heavy quark diffusion transport parameter of the QGP medium along with its temperature dependence. Figure 4.7 (right) shows how the v_2 measurement can be further extended to the tens of GeV range, where the path-length differential energy loss of the b-quark is probed.

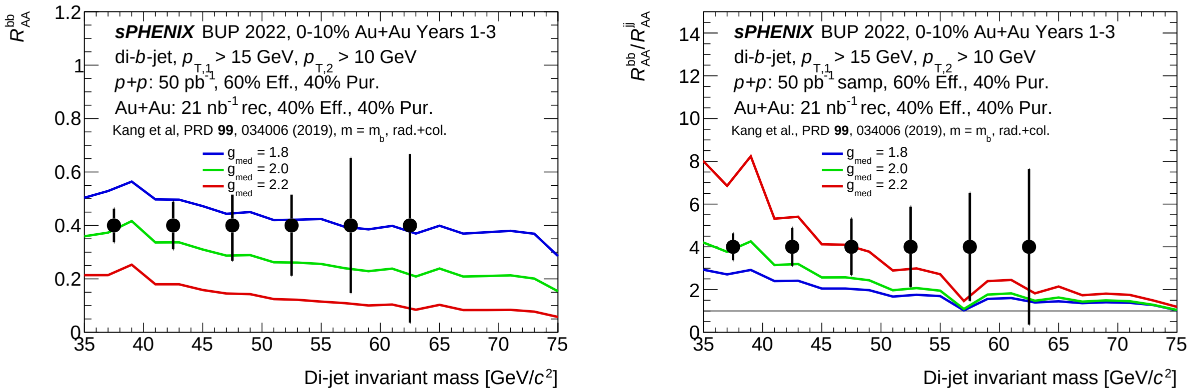

Figure 4.8: Projected statistical uncertainties of nuclear modification for back-to-back b-jet pairs (left) and b-jet-light-jet super-ratio (right) along with pQCD calculations from Ref. [21]

With the large acceptance and multi-observable capability, the sPHENIX experiment is well positioned to explore new heavy-flavor correlations. Recently, the invariant mass of back-to-back heavy-flavor jet pairs has been shown to be a promising experimental observable for studying the propagation of quarks in the QGP [21]. The 3-year projection for the nuclear modification of the invariant mass for back-to-back b-jet pairs and the b-jet-light-jet super-ratio is shown in Figure 4.8. Comparing to predictions based on 10% variation of the coupling parameter, g^{med}, the sPHENIX data will place stringent constraints on the b-quark coupling to the QGP under this model. The large sample for the heavy-flavor hadron and jet also enables a correlation study for heavy-flavor meson pairs, heavy-flavor meson-jet correlation, and other jet-jet observables that are being studied by the collaboration [22, 23];

The large yield of identified b-jets will also allow for differential studies of their properties. As one example, the left panel of Figure 4.9 shows the expected statistical uncertainties on a measurement of the sub-jet splitting fraction z_g in 15–30 GeV b-jets in p+p and 0–10% Au+Au events. We note that b-jets can likely be measured to significantly lower p_{T} than inclusive jets, since the b-tagging requirements strongly suppress underlying event fluctuation jets. The right panel of Figure 4.9 shows the Au+Au/p+p ratio compared to one expectation of the (large) medium modifications [24].

Finally, recent RHIC and LHC data indicate significant enhancement of the Λ_c baryon to D^0 meson production ratio in $p+p$, $p+A$ and A+A collisions [25]. However, the data at RHIC is still sparse and the reference Λ_c/D ratio in $p+p$ collision is missing at RHIC energies, while the current model predictions differ significantly. As shown in Figure 4.10, sPHENIX will enable the first measurement of the Λ_c/D in $p+p$ collisions at RHIC and provide the high precision heavy ion data to quantitatively understand the enhancement of the charmed baryon/meson production ratio and therefore charm hadronization in the quark-gluon plasma.

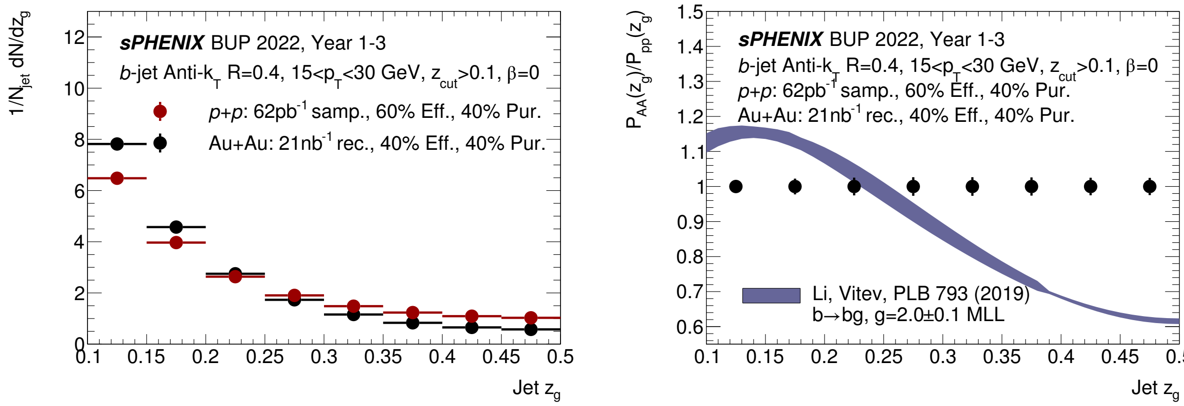

Figure 4.9: Projected statistical uncertainties for the subjet splitting fraction z_g for b-jets in p+p and Au+Au (left) and the Au+Au/p+p ratio compared to the expectation from a pQCD calculations from Ref. [24].

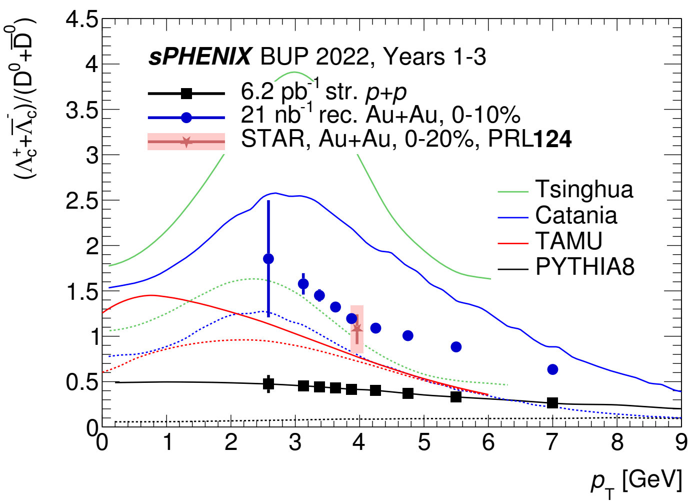

Figure 4.10: Statistical projections of Λ_c/D ratio for both central Au+Au and $p+p$ collisions. This projection is compared with the recent publication from the STAR collaboration in the central Au+Au collisions [25] (red point), model calculations of this ratio in the Au+Au collisions (colored curves), and the PYTHIA8 tunes for the $p+p$ collisions (black curves).

4.4 Cold QCD and p+A Physics

The sPHENIX detector, primarily designed to study the quark-gluon plasma with jet, photon and heavy-flavor probes with its trigger and high DAQ rate capabilities, will also provide key opportunities for cold QCD and small system collectivity measurements. These include a broad range of physics measurements, including measurements of jet, hadron and heavy flavor collective motion, measurements with transversely polarized beams, and studies of transverse momentum dependent (TMD) effects and hadronization in $p+p$ and $p+A$ collisions.

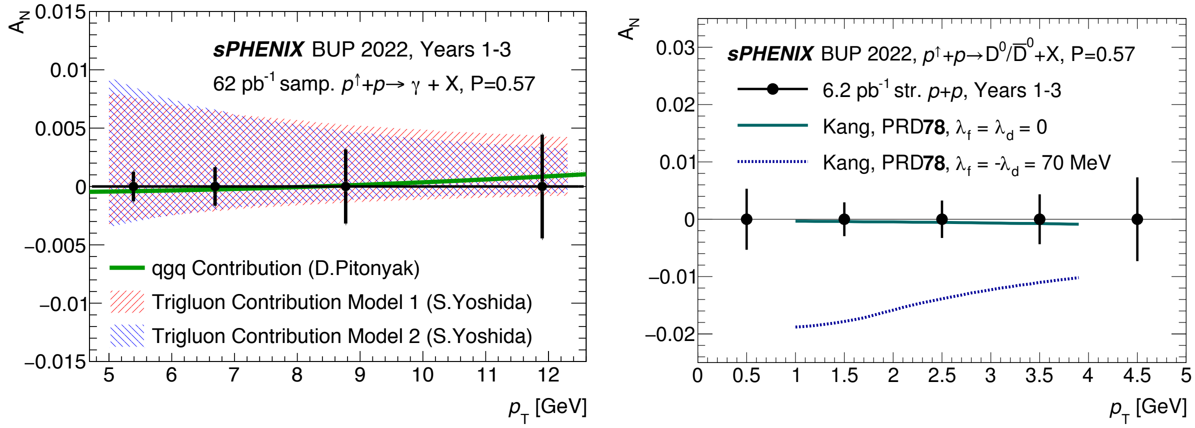

Figure 4.11: Left: Projected statistical uncertainties for direct photon A_N. Right: Statistical projections of transverse spin asymmetry for the D^0 mesons for Year-2, which is compared with various scenarios modeled in the twist-3 model in [26].

4.4.1 Transverse Spin Measurements

In recent years, transverse spin phenomena have gained substantial attention. The nature of significant transverse single spin asymmetries (TSSAs) in hadron collisions, discovered more than 40 years ago at low center-of-mass energy ($\sqrt{s} = 4.9$ GeV), and then confirmed at higher energies up to $\sqrt{s} = 510$ GeV and $p_T \sim 7$ GeV at RHIC, has not yet been fully understood. Different mechanisms have been suggested to explain such asymmetries, involving initial-state and final-state effects, in the collinear or transverse-momentum-dependent (TMD) framework. These descriptions have deep connections to nucleon partonic structure and parton dynamics within the nucleon, as well as spin-momentum correlations in the process of hadronization.

The TSSAs in direct photon and heavy-flavor production probe the gluon dynamics within a transversely polarized nucleon, described by the tri-gluon correlation function in the collinear twist-3 framework, which is connected with the gluon Sivers TMD parton distribution function (PDF), thus far poorly constrained. The Sivers function correlates the nucleon transverse spin with the parton transverse momentum.

The projected uncertainties for the midrapidity direct photon TSSAs compared to theoretical calculations are shown in the left panel of Figure 4.11. The direct photon sample here will be collected with an EMCal-based high-energy cluster trigger. The new capability of the sPHENIX streaming DAQ (detailed in Section C.2) enables a high precision measurement of D^0 TSSA in the mid-rapidity region as shown in the right panel of Figure 4.11.

Another interesting channel related to the Sivers effect is the inclusive jet TSSA, which has not yet been measured at central rapidity. sPHENIX can provide high precision measurements with uncertainties on the level of a few times 10^{-4}. While the opposite sign contribution of up and down quarks to Sivers asymmetry is expected to suppress the measured TSSA, tagging the leading hadron charge will preferentially enhance the contribution from fragmenting up or down quarks, and therefore will enable the flavor-separated measurements in the central rapidity kinematics. Such measurements are complementary to the future jet TSSAs at the EIC, and are also expected to have opposite signs due to the properties of the gauge links involved in the processes. This provides a fundamental test of QCD factorization in $p+p$ and $e+p$ interactions.

Dijet measurements allow for direct access to parton intrinsic transverse momentum k_T. Again, charge-tagged jets will enhance the effect from either up or down quarks, which otherwise will be essentially cancelled out. Recent STAR preliminary results showed a nonzero effect for charge-tagged jets. As a dedicated detector for jet and photon measurements, sPHENIX is expected to significantly contribute to dijet measurements, and to extend them to photon-jet measurements which can isolate the quark-gluon scattering process at leading order, thus giving access to the gluon Sivers effect.

Another possible origin of the observed TSSAs is the Collins mechanism, which correlates the transverse polarization of a fragmented quark to the angular distribution of hadrons within a jet. This gives access to the transversity distribution in the proton, which can be interpreted as the net transverse polarization of quarks within a transversely polarized proton. Along with the unpolarized PDF and helicity PDF, transversity is one of three leading-twist PDFs, least known at the moment. The integral in x over the valence quark transversity distribution defines the tensor charge, a fundamental value calculable in lattice QCD, therefore enabling the crucial comparison of experimental measurements with *ab initio* theoretical calculations.

Measuring angular distributions of dihadrons in the collisions of transversely polarized protons, couples transversity to the so-called "interference fragmentation function" (IFF) in the framework of collinear factorization. The IFF describes a correlation between the spin of an outgoing quark and the angular distribution of a hadron pair that fragments from that quark. A comparison of the transversity signals extracted from the Collins effect and IFF measurements will explore questions about universality and factorization breaking.

The first non-zero Collins and IFF asymmetries in $p+p$ collisions have been observed by the STAR collaboration at midrapidity [27, 28] and shown to be invaluable to constrain the transversity distribution. sPHENIX, with its excellent hadron and jet calorimetric trigger capabilities coupled with its high-rate DAQ capabilities, is expected to deliver high-statistics samples for both Collins and IFF asymmetries. The sPHENIX capability to collect a significant data sample with streaming readout will allow us to extend the charged dihadron measurements for IFF asymmetries from the barrel region ($|\eta| < 1$) to more forward kinematics up to $\eta = 2$.

4.4.2 Transverse Spin: $p+p$ vs $p+A$

Unique opportunities are present with polarzied $p^{\uparrow}$+A collisions at RHIC to study spin effects in a nuclear environment. These studies provide new insights into the origin of the observed TSSAs and a unique tool to investigate the rich phenomena behind TSSAs in hadronic collisions. TSSAs measured in polarized $p^{\uparrow}$+A collisions moreover offer a new approach to studying small-system collisions, in which numerous surprising effects have been observed in recent years.

First RHIC results from the 2015 RHIC run showed a puzzling evolution of the TSSA from $p^{\uparrow}+p^{\uparrow}$ to $p^{\uparrow}$+Al and then $p^{\uparrow}$+Au. While STAR's preliminary result for π^0 asymmetry in forward rapidity (with $0.2 < x_F < 0.7$) showed no significant nuclear dependence, PHENIX's positively charged hadron asymmetries in the intermediate rapidity range (with $0.1 < x_F < 0.2$) discovered a strong nuclear dependence in the TSSA, from $A_N \sim 0.03$ in $p^{\uparrow}+p^{\uparrow}$ collisions to a value consistent with zero in $p+$Au collisions. No clear explanation for such a behavior has been offered at the moment.

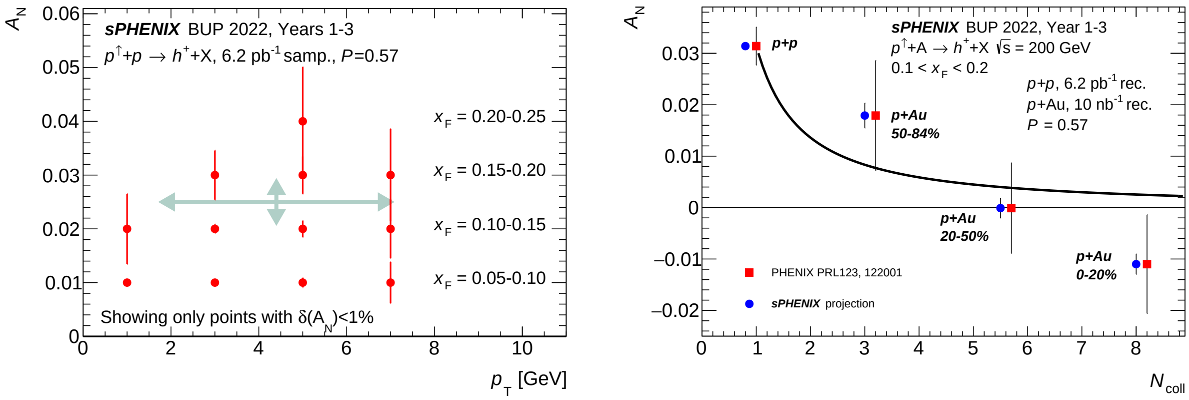

Figure 4.12: (Left) Projected statistical uncertainties for h^+ A_N in p+p collisions, for data collected with streaming readout; green arrows indicate the statistical uncertainty and p_T coverage of the single PHENIX data point (with $0.1 < x_F < 0.2$). (Right) Projected statistical uncertainties as a function of the average number of nucleon-nucleon collisions in each centrality bin.

Obviously, more data, differentiated in p_T and x_F, would be highly desirable. sPHENIX is able to collect much more data in this channel, with fine binning, which is expected to provide crucial information on the nature of TSSAs in hadronic collisions and on understanding of the spin probe—nucleus interaction, a novel topic directly associated with RHIC's unique ability to collide polarized protons with nuclei.

The left panel Figure 4.12 shows the projected uncertainties for sPHENIX, based on minimum bias data collected with the streaming readout. The sPHENIX tracking system will provide us with charged hadron measurements in the pseudorapidity range up to $\eta = 2$, which overlaps with the PHENIX range, where the strong nuclear effect was observed ($1.2 < \eta < 2.4$).

In addition, sPHENIX can explore the nuclear dependence of TSSAs. The first RHIC p+Al and p+Au runs with transversely polarized protons in 2015 brought a number of surprising results, among them the strong nuclear suppression of the charged hadron TSSA in p+Au collisions compared to p+p collision in the intermediate rapidity region of $\eta = 1.2 - 2.4$ [29], discovered by PHENIX, while more forward measurements of π^0 TSSA, as reported by STAR, showed only weak nuclear dependence [30]. Such behavior of TSSA in p+Au collisions remains unexplained. The data to be collected by sPHENIX in p+p and p+Au collisions would considerably improve the precision of the measurements, as shown in the right panel of Figure 4.12. By allowing for a measurement of TSSAs with fine binning in p_T and x_F in extended ranges, these would provide valuable information for studying rich phenomena behind TSSA in hadronic collisions, and utilize RHIC's unique capabilities to collide high energy polarized protons and heavy nuclei.

Other measurements (e.g. Collins and IFF asymmetries) will also be compared between $p+p$ and $p^{\uparrow}+$Au systems and may bring new surprises.

4.4.3 Unpolarized Measurements

A number of measurements that do not require beam polarization are planned in $p+p$ and $p+A$ collisions. Figure 4.13 demonstrates the kinematic reach for inclusive jet, photon, and charged

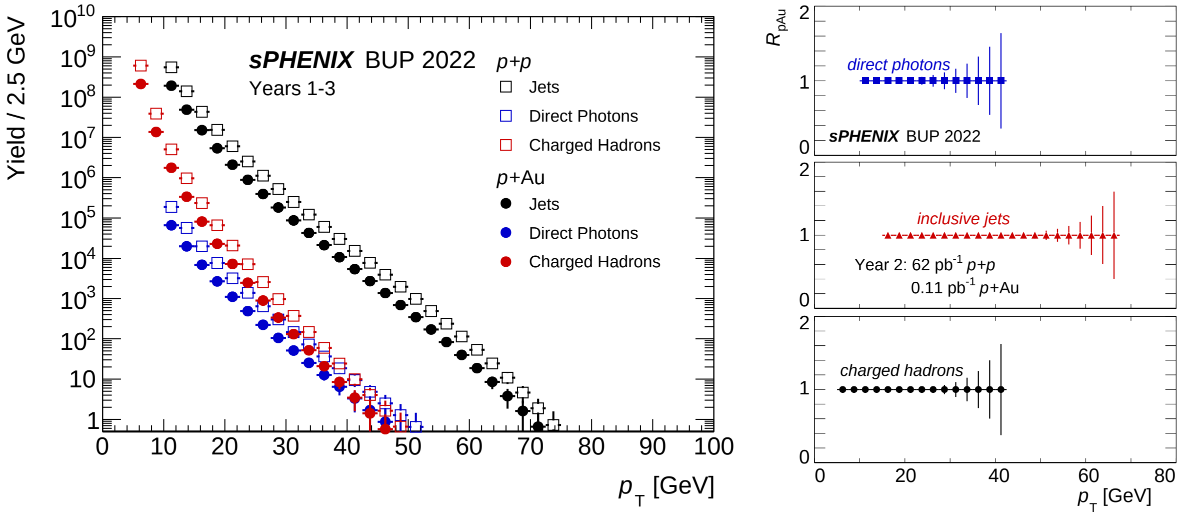

Figure 4.13: Projected total yields (left) and R_{pA} (right) for jets, photons, and charged hadrons in centrality-integrated p+Au events, for the first three years of sPHENIX data-taking.

hadron measurements in this system via the expected total yields and the projected uncertainties in the nuclear modification factor R_{pA}. sPHENIX will deliver sufficient data to measure jets out to ~ 70 GeV, and charged hadrons and direct photons out to ~ 45 GeV.

Hadronization studies will be performed with hadron-in-jet measurements, multi-differential in momentum fraction z of the jet carried by the produced hadron, in the transverse momentum j_T of the hadron with respect to the jet axis, and in the angular radial profile r of the hadron with respect to the jet axis. This includes studies for both light quark and heavy quark hadrons. Comparison of $p+p$ and $p+$A collisions will provide information on the nuclear modification of hadronization processes. Measurements performed by PHENIX of non-perturbative transverse momentum effects and their nuclear modifications in back-to-back dihadron and photon-hadron correlations, will be extended to dijet and photon-jet measurements in sPHENIX. These measurements will help to separate the effects associated with intrinsic parton momentum k_T in the nucleon or nucleus and fragmentation transverse momentum j_T. These correlation measurements may also help to probe theoretically predicted factorization breaking effects within the transverse-momentum-dependent framework. Upsilon and J/ψ polarization measurements will shed further light on heavy quarkonium production mechanisms.

4.4.4 Collective behavior in p+A collisions

Over the last decade one of the exciting areas of heavy ion physics relates to collectivity in small systems – see Ref. [31] for a recent review. In $p+p$ and p+Pb collisions at the Large Hadron Collider (LHC) and p+Au, d+Au, ^{3}He+Au collisions at RHIC, there is strong evidence for the translation of initial geometry deformations in flow harmonics.

Correlations with light particles. Using the 10%-streaming readout, even a modest p+Au run would provided enormous statistics for track-only analyses. As an example of what this provides buys, Figure 4.14 shows the projected statistical uncertainties for the elliptic flow cumulants in p+Au

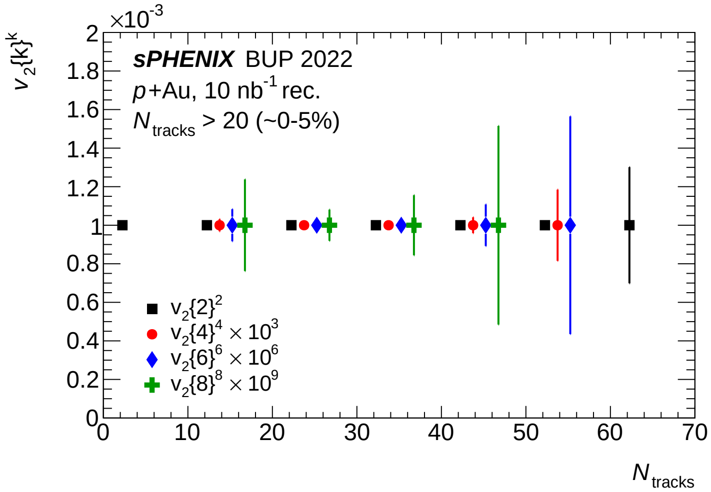

Figure 4.14: Projected statistical uncertainties for charged hadron cumulants up to eighth order. These results are obtainable in the 24 and 28 cryo-week scenarios.

collisions as a function of track multiplicity. For the 0-5% most central selection, one would have precision measurements up through the 8th order cumulant. These measurement can provide qualitatively new insights on multi-particle collectivity that are hinted at via the PHENIX published d+Au cumulants, with second, fourth, and very modest sixth orders [32].

Additionally, the PHENIX published results in Nature Physics [33] on elliptic and triangular flow have generated significant interest in the field, which have now been corroborated with additional analysis checks [34]. There have since been multiple STAR preliminary results that generally confirm the elliptic flow but have a significantly different result for triangular flow in $p+$Au and d+Au collisions. While publication of the STAR results would be a positive step forward, a parallel way to proceed would be to measure both short-range and long-range correlations in the same experiment with high statistics. sPHENIX will have the same tracking coverage as the STAR barrel detector and a $p+$Au run would result in much higher statistics data samples. The sPHENIX Event Plane Detector (recently awarded an NSF MRI and under construction) enables PHENIX-style long-range correlations as well. Thus, this $p+$Au data set in sPHENIX is likely to further elucidate collectivity in small systems and the relevant sub-nucleon geometry.

Heavy flavor collectivity. Heavy flavor (charm and bottom) quarks are an excellent probe of quark-gluon plasma effects. Once produced in early high-Q^2 processes, the flavor is conserved and thus the quarks get dragged and diffused through the medium. Measurements of charm and bottom hadrons and bottom-tagged jets in Au+Au collisions comprise a major part of the sPHENIX program as detailed in Section 4.3. Recent measurements of collectivity in small systems has increased the focus on measurements of these heavy quarks in p+Au and p+Pb collisions at RHIC and the LHC. Measurements of significant D meson elliptic flow v_2 in p+Pb collisions by CMS at the LHC [35] is intriguing since the transverse momentum distribution appears mostly unmodified relative to $p+p$ collisions [36]. Even muons from charm decays have a significant v_2 in high multiplicity $p+p$ collisions at the LHC, though muon from bottom decays are consistent with zero [37].

sPHENIX can make comparable precision measurements in a $p+$Au run of both the transverse

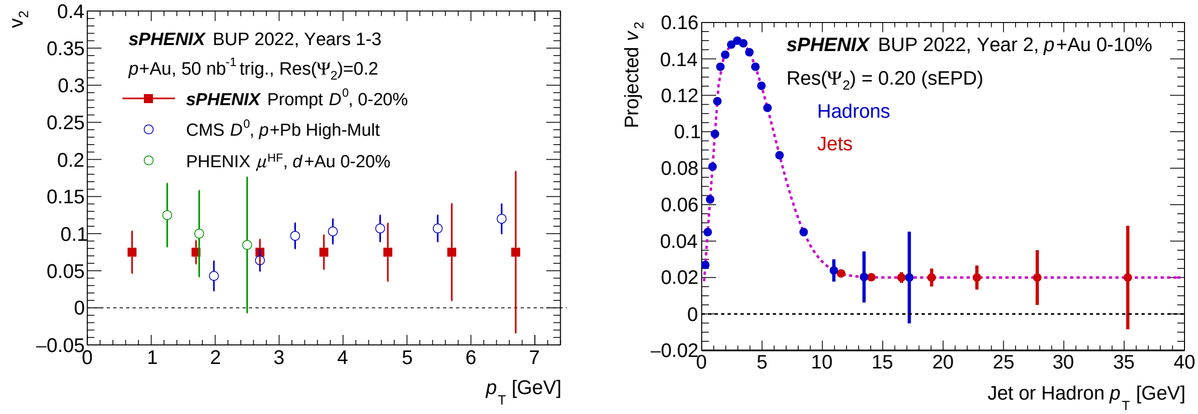

Figure 4.15: Left: sPHENIX projected statistical uncertainties for fully-reconstructed prompt D^0 meson v_2 as a function of transverse momentum in $p+$Au 0-20% central collisions, compared to v_2 for heavy flavor muons from PHENIX and D^0's from CMS [35]. Right: Projected sPHENIX statistical uncertainties for charged hadron and reconstructed jet v_2 versus p_T in 0-10% central p+Au collisions.

momentum spectrum and the elliptic flow. As an example, the left panel of Figure 4.15 shows the projected statistical uncertainties for fully-reconstructed prompt D^0 meson v_2 as a function of transverse momentum from a 2024 $p+$Au run, compared to the previous measurement in d+Au collisions with PHENIX, and the measurement by CMS. Measurements at both RHIC and the LHC are important to constrain explanations for these anisotropies.

Jets and high-p_T hadrons. A critical baseline for understanding jet quenching effects in nucleus-nucleus collisions is to measure the same observables in $p+$Au collisions. Originally back in 2003, the d+Au run was motivated by the desire to isolate so-called "cold nuclear matter" effects from jet quenching. Since then, the measurements have taken on the additional burden of trying to cleanly identify potential jet quenching effects in small collision systems.

The ATLAS experiment at the LHC has measured elliptic flow coefficients v_2 for charged hadrons in the high p_T region 10–50 GeV in p+Pb collisions [38], with a quantitatively similar p_T dependence to this same region in Pb+Pb collisions. In Pb+Pb collisions this azimuthal anisotropy is thought to result from differential jet quenching with respect to the collision geometry. However, currently no jet quenching is observed in p+Pb collisions, and so this is challenging as a common explanation in p+Pb. sPHENIX will be able to measure elliptic flow coefficients for charged hadrons and reconstructed jets up to high p_T, as shown in the right panel of Figure 4.15. As part of a suite of $p+$Au hard process measurements by sPHENIX, one will have excellent constraints on explanations of this phenomena.

Chapter 5

Summary

sPHENIX will be the first new collider detector at RHIC in over twenty years, performing very high precision studies of jet production, jet substructure and open and hidden heavy flavor over an unprecedented kinematic range at RHIC. The experiment is a specific priority of the DOE/NSF NSAC 2015 Long Range Plan and will play a critical role in the completion of the RHIC science mission by enabling qualitatively new measurements of the microscopic nature of quark-gluon plasma. sPHENIX is distinguished by high rate capability and large acceptance, combined with high precision tracking and electromagnetic and hadronic calorimetry.

The effort to construct the experiment is officially underway, with the DOE MIE project having been granted PD-2/3 approval in September 2019. The first year of data taking will be 2023; the final year of sPHENIX operations is foreseen for 2025 as dictated by BNL's reference schedule for the EIC project.

Each run in this three-year period plays a critical role in fulfilling the sPHENIX science mission outlined in the NP Long Range Plan:

- Year-1 serves to commission all detector subsystems and full detector operations, and to validate the calibration and reconstruction operations essential to delivering the sPHENIX science in a timely manner. Year-1 will also allow collection of a Au+Au data set enabling sPHENIX to repeat and extend measurements of "standard candles" at RHIC.
- Year-2 will see commissioning of the detector for $p+p$ collisions and collection of a large $p+p$ reference data set, as well as a large $p+$Au data set for studies of cold QCD.
- Year-3 is focused on collecting a very large statistics Au+Au data set for measurements of jets and heavy flavor observables with unprecedented statistical precision and accuracy.

The sPHENIX collaboration is excited for the unique physics opportunities enabled by this run plan and to positively conclude the scientific mission of RHIC.

Appendix A

Beam Use Proposal Charge

The charge from the Associate Laboratory Director Haiyan Gao was received by the sPHENIX Spokespersons on March 21, 2022. The charge is included below.

STAR: Beam Use Requests for Runs 23-25

sPHENIX: Beam Use Requests for Runs 23-25

CeC: Beam Use Requests

The Beam Use Requests should be submitted in written form to PAC by May 6, 2022

The BURs should be based on the following number of cryo-weeks. The first number is the proposed RHIC run duration for scenario 1 and the second number corresponds to optimal duration (scenario 2) presented to the DOE-ONP in BNL's FY24 Lab Managers' Budget Briefing:

2023: 24 (28)

2024: 24 (28)

2025: 24 (28)

Note the eventual running cryo-weeks for each run will depend on the final budget guidance for that year so it can be lower than 24 weeks.

Presentations:

STAR: Report on Run 2022, update on BES-II, small systems and spin physics analyses, and the latest development regarding the Isobar results.

CeC X: Results from Run 2022

PHENIX: Update on ongoing analysis efforts and data archiving efforts

sPHENIX: Installation status and schedule including TPOT status, commissioning, computing plan and readiness for data taking.

Written report from the PAC is expected within two weeks after the meeting.

Appendix B

Crossing Angle

The original C-AD projections for Au+Au 200 GeV collision rate as a function of time-in-store for the years 2023, 2025, and 2027 are shown in Figure B.1 (left). The black curves are the collision rate for interactions at any longitudinal z vertex position, while the red curves are the collision rate for interactions with $|z| < 10$ cm. The magenta curve corresponds to the design specified 15 kHz sPHENIX Level-1 trigger accept rate. These projections are with zero crossing angle between the beams.

The sPHENIX optimal acceptance for the inner tracking detectors is with collisions within $|z| < 10$ cm. Thus, it is clear that a majority of the collisions in this running mode with zero crossing angle have highly sub-optimal tracking acceptance. In principle these collisions far outside the optimal region (i.e. $|z| > 10$ cm) still could be used for calorimeter-only physics measurements (e.g. high p_T photons and calorimetric jets) – however, one would not have good acceptance to measure jet fragmentation functions, or medium response via tracks in these events. There is a significant down side to the very large collision rate outside of $|z| < 10$ cm. These collisions still leave hits in the TPC and thus substantially increase ion back-flow (IBF) and fluctuations in the IBF. This additional charge is corrected for but at the same time gets more and more challenging and eventually degrades the track momentum resolution and track finding efficiency. Additionally, components of sPHENIX including the calorimeter silicon photo-multipliers (SiPMs) are susceptible to radiation damage over time. These additional collisions significantly increase the overall time-integrated radiation load on the detector.

Therefore, after detailed discussions with C-AD, sPHENIX plans to run with a nominal beam crossing angle of 2 milliradians in Au+Au collisions. C-AD has included collision rate information at beam crossing angles of 0, 1, and 2 milliradians in their projections document. Figure B.1 (right) shows the collision rate as a function of time in store for a nominal 2 milliradian crossing angle. There is a modest reduction in collision rate within $|z| < 10$ cm; however, it still exceeds the 15 kHz Level-1 accept rate throughout the store. What is most noticeable is the reduction by almost a factor of three in total collision rate. This effectively translates into a factor of three lower radiation load on the detector and three times lower charge deposition in the TPC. Small optimizations around the 2 milliradian value may be possible; for the purposes of this document we have consistently used this 2 milliradian crossing angle for all projections.

Similar issues of acceptance and radiation load / IBF have to be balanced for p+p and p+Au

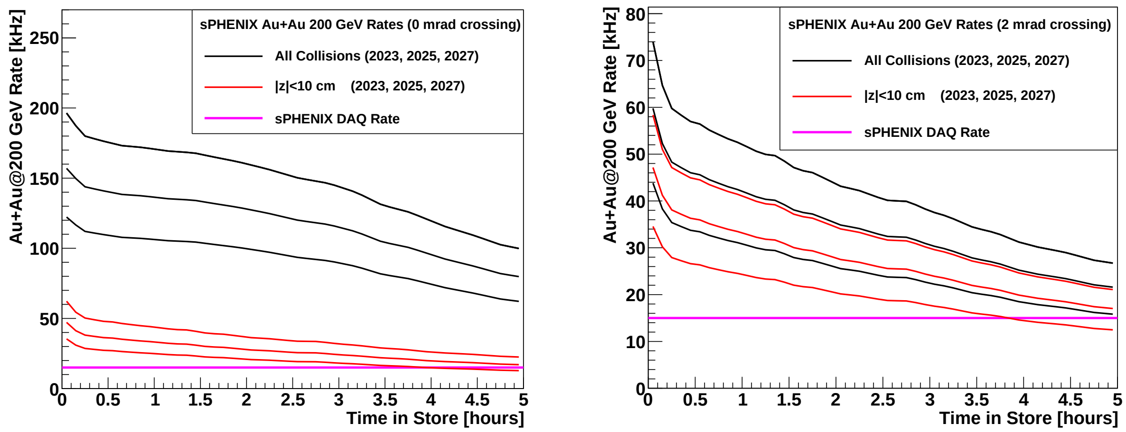

Figure B.1: (left) Estimated Au+Au at 200 GeV collision rate as a function of Time in Store for all collisions (black) and collisions within $\pm$ 10 cm (red). The bottom to top set of curves in each color are for the C-AD projections in their document corresponding to 2023, 2025, 2027. Also shown as a magenta line is the sPHENIX data acquisition rate of 15 kHz for reference. These projections are with zero crossing angle between the beams. (right) The same calculated quantities are shown for a 2 milliradian crossing angle between the beams.

running. The current proposal is to run with the same 2 milliradian crossing angle for these systems as well. We highlight that in p+p and p+Au running, the larger collision rate with lower track multiplicities may lead to small IBF fluctuations since the collisions are spread out in z vertex and there are more random chances to average out relative to a smaller number of Au+Au collisions with highly variable multiplicity. It may be that there is thus a somewhat smaller crossing angle that will be optimal for the smaller collision systems.

B.1 Summary of Projected Luminosities

Wolfram Fischer and C-AD have provided a MATHEMATICA notebook for estimating the collision rate and z-vertex collision distribution as a function of beam crossing angle. After confirming values with C-AD, we include the generated set of results here for completeness, see Figures B.2, B.3, and B.4.

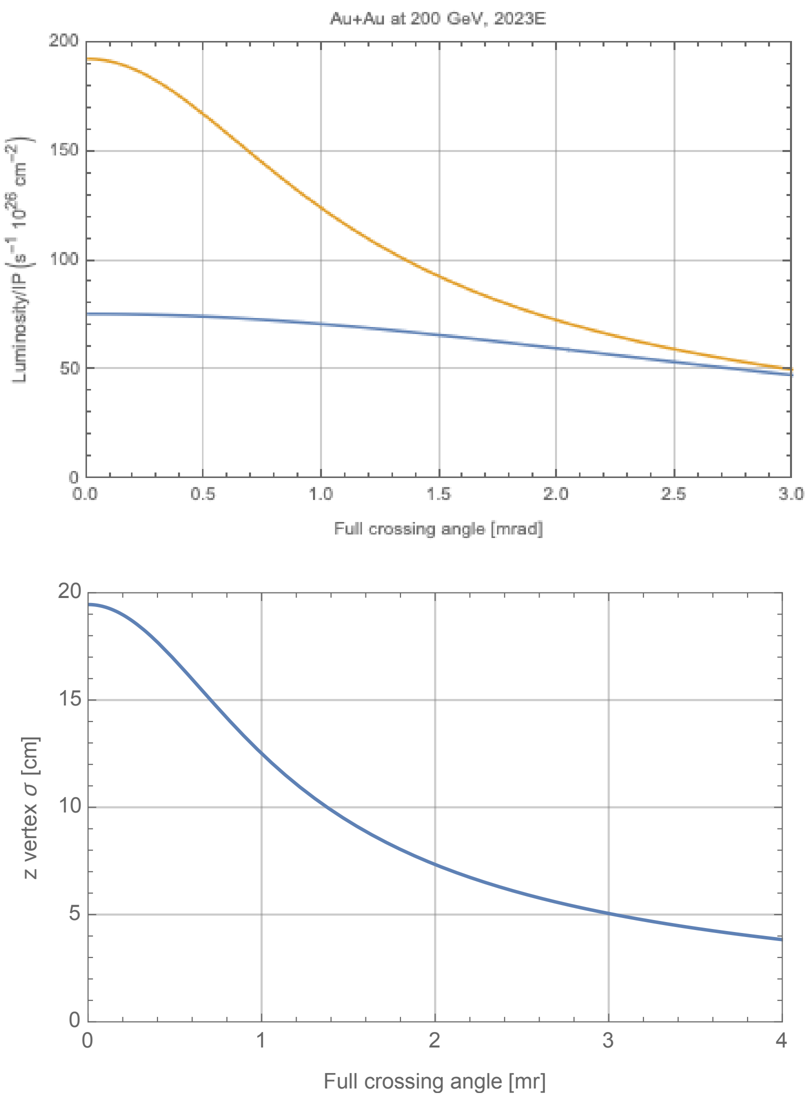

Figure B.2: C-AD MATHEMATICA file generated Au+Au collision luminosity (left) and z-vertex Gaussian σ (right) as a function of beam crossing angle.

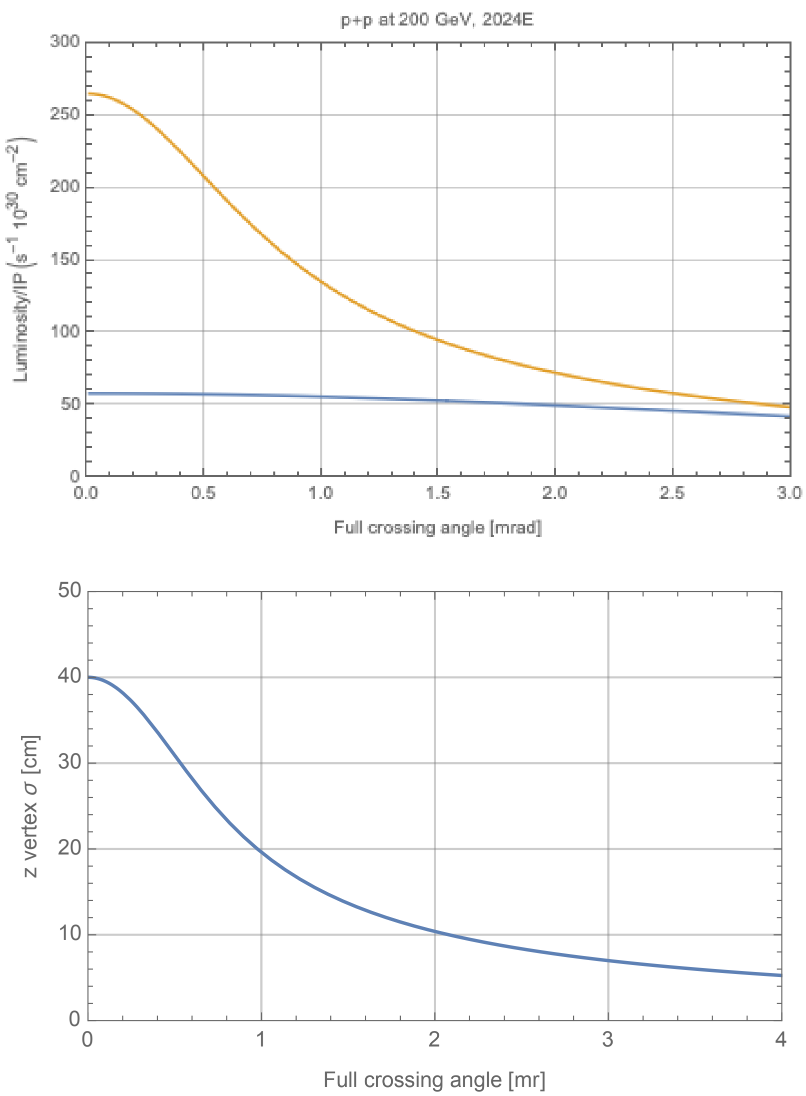

Figure B.3: C-AD MATHEMATICA file generated $p+p$ collision luminosity (left) and z-vertex Gaussian σ (right) as a function of beam crossing angle.

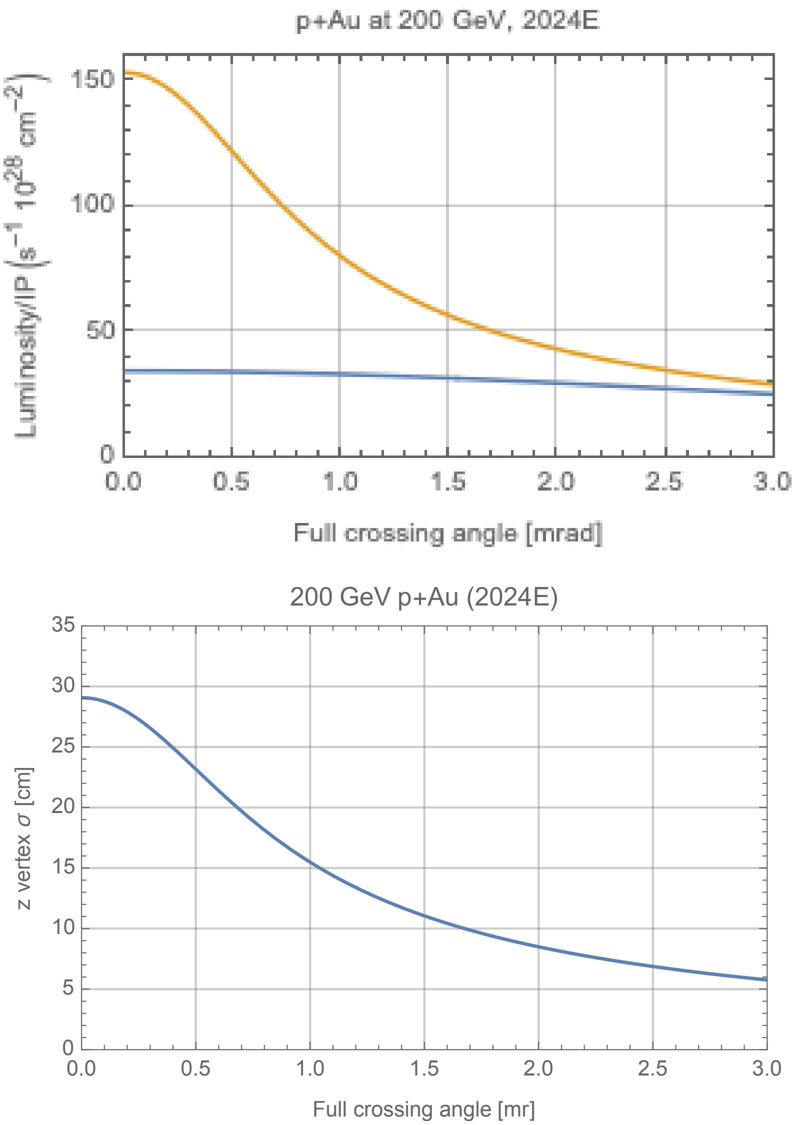

Figure B.4: C-AD MATHEMATICA file generated p+Au collision luminosity (left) and z-vertex Gaussian σ (right) as a function of beam crossing angle.

Appendix C

Upgrades of the sPHENIX Readout

In this appendix we detail the potential of two modest cost upgrades of the sPHENIX data acquisition and readout system to significantly enhance the original physics program. The first is a streaming (rather than triggered) readout of the tracking detectors (MVTX, INTT, and TPC) which could be available at 10% capacity for the 2024 run and at 100% capacity for running in 2026–2027 should that opportunity arise. The second is a demultiplexing of the readout electronics for the calorimeter system which would enable a doubling of the Level-1 trigger rate for these detectors from 15 kHz to 30 kHz. This upgrade could be available for running in 2026–2027. We detail these two options in the sections below.

C.1 Streaming Readout Upgrade for the sPHENIX trackers

The nominal sPHENIX DAQ model assumes calorimeter-based Level-1 triggers for $p+p$ and $p+$Au data taking. Many sPHENIX observables, such as photons and jets, leave clear signatures in the calorimeter system that can be used to produce a sufficiently selective Level-1 trigger. However, further physics opportunities are present only in the non-triggerable data stream. One example is low-p_T open heavy-flavor hadrons that decay hadronically and leave relatively small signals in the calorimeters compared to the background coming from the underlying event. These physics channels cannot be efficiently collected via calorimeter triggers, which have too high an energy threshold. One would likely allocate 1-5 kHz of the full 15 kHz of the sPHENIX trigger bandwidth for this type of program in minimum bias $p+p$ or $p+$Au. This translates into rather limited statistics for these rare low-p_T heavy-flavor signals as quantified in Table C.1 (left column).

The tracking detectors for the sPHENIX experiment all support streaming readout mode, that is where the digitization and readout of the data off the detector does not require Level-1 trigger information as shown in Figure C.1. The currently envisioned nominal data taking mode is where the data acquisition selects the time-slice of the tracker data that corresponds to the calorimeteric-triggered event and saves those time-slices to the output raw data file. A streaming readout upgrade in the data acquisition (DAQ) firmware and software is being developed by the collaboration to record a tunable fraction of the tracker data stream on top of the calorimeteric-triggered events, which can vastly increase the fully recorded minimum bias collision event in the full tracking system.

This hybrid trigger-streaming DAQ is particularly efficient in the sense that the number of recorded events per gigabyte of raw data is optimized. By extending the tracker data recording time window immediately following a calorimeteric-triggered event and completing the partially recorded off-time collisions in the long integration time window of the MVTX and TPC detectors, one captures additional interactions most efficiently. From an analysis point of view, this is an elegant solution as it avoids any trigger selection bias which would be quite complicated for rare and weak signals such as hadronically decayed heavy-flavor hadrons. The effect of this upgrade can be quantified as shown in Figure C.2, where a 50% increase in the data volume column allows for recording 10% of **all** minimum biased collisions, an increase by two to three orders of magnitude as detailed in Table C.1 (right columns).

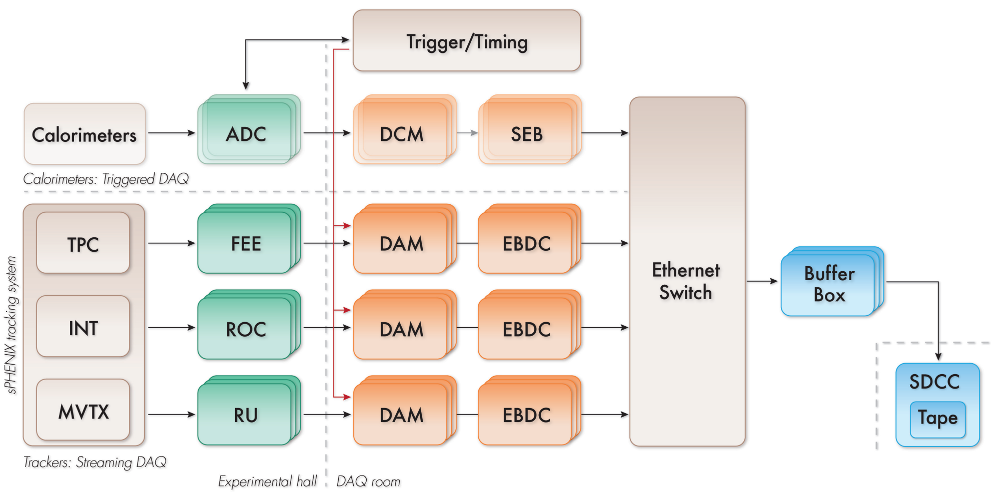

Figure C.1: The hybrid DAQ structure of the sPHENIX tracking detectors, in which all three detectors are read out in a streaming mode. The output of the tracker data streams are throttled appropriately to be in synchrony with calorimeter triggers. Additional tracker data can also be streamed, providing an opportunity to record minimum bias collisions beyond those coming from calorimeter-triggered events.

C.1.1 Hybrid Trigger-Streaming Readout in 2024

In the 2024 run, we plan to implement the first streaming readout DAQ for the tracking detectors to record 10% of the delivered luminosity in addition to the calorimeteric-triggered events. The data rate and data volume is dominated by the time projection chamber which is studied in Figure C.2. With the introduction of the beam crossing angle, the expected data rate with the 10% streaming readout would be much lower than the design specifications and the previous data volume estimates with zero crossing angle assumed in the 2019 sPHENIX computing plan [39]. The reason is simply because with the 2 milliradian crossing angle there are far fewer collisions outside of $|z| < 10$ cm that would have still caused hits in the TPC that would have been recorded.

The physics gain is significant, that includes the $p+p$ reference data for the D^0 R_{AA} and the Λ_c/D^0

		Year-2024, triggered DAQ per-1kHz M.B. trigger	Year-2024, w/ str. tracker	Year 2026 w/ str. tracker
M.B. p+p	Data Mode	Each 1k Hz M.B. trigger w/ 4×10^{-4} of M.B. coll. triggered	10% M.B. events str. recorded	100% M.B. events str. recorded
	Stats	1 Billion M.B. evts 0.026 pb^{-1} recorded	250 Billion M.B. evts 6.2 pb^{-1} recorded	3.2 Trillion M.B. evts 80 pb^{-1} recorded
Physics Reach	$\mathrm{B} \rightarrow \mathrm{D}^0 \rightarrow \pi\mathrm{K}$ R_{AA} ref.	620 evts	150k evts	2M evts
	$\mathrm{D}^0 \rightarrow \pi\mathrm{K}$ pair Diffusion of c+$\bar{c}$	620 evts	150k evts	2M evts
	$\Lambda_c \rightarrow \pi\mathrm{K}p$ Charm hadronization	1.3k evts	310k evts	4M evts
	Prompt $\mathrm{D}^0 \rightarrow \pi\mathrm{K}$ Tri-Gluon Corr. via TSSA	0.2M evts	50M evts	0.6B evts

Table C.1: Statistical reach for HF p+p events by channel in different data taking periods and modes, including streaming readout of the tracker.

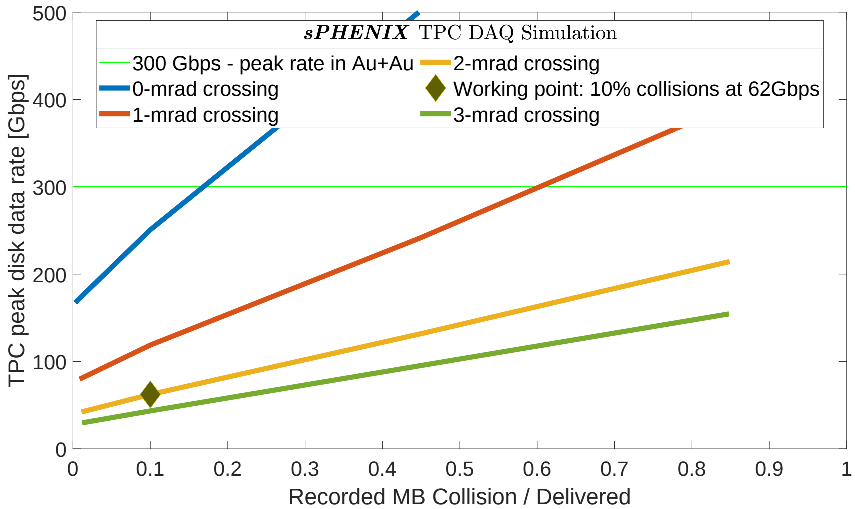

Figure C.2: Choice of operation point between the peak TPC data logging rate and the fraction of M.B. p+p collision recorded. The green horizontal line denotes the peak data logging rate for Au+Au collisions. At similar logging rate and without the beam crossing angle, a minimum of 10–20% of $p+p$ M.B. collisions can be streamed to the raw data file as denoted by the solid blue curve. In the case that a beam cross angle is introduced (red, orange and green curves) the overall data rate can be significantly reduced. The default work point in the 2024 run is with 2 mrad beam crossing angle and record 10% of collisions at 62 Gbps data rate as denoted by the diamond point.

ratio both of which are critical for the systematic control in understanding the Au+Au data as discussed in Section 4.3. In addition, since the $p+p$ beam is transversely polarized, the single spin asymmetry in the D^0 channel can be measured to gain access of tri-gluon correlation [26, 40], which is further discussed in Section 4.4. All aforementioned physics gains would be first measurements at RHIC and uniquely enabled by the streaming DAQ of the sPHENIX trackers.

C.1.2 Full streaming Readout for Potential 2026–2027 Running

If RHIC runs in 2026 and/or 2027 become available, we would augment the initial DAQ to be able to stream *all* of the data from the sPHENIX tracking detectors for *all* collision species. The curves in Figure C.2 show that as the fraction of streaming data is increase, the TPC data rate increases, and a fully streamed DAQ would have imply a data rate wsignificantly higher than the 2024 working point, shown as a black diamond in the figure. However, assuming even a small beam crossing angle, this data rate would still be below the 300 Gbps bandwidth limit of the full readout system neotiated with the RHIC computing facility. At the expense of a somewhat higher data volume, a full streaming readout of the trackers allows another order of magnitude improvement in the recorded $p+p$ and $p+A$ statistics, whose impact is further quantified in Chapter D.

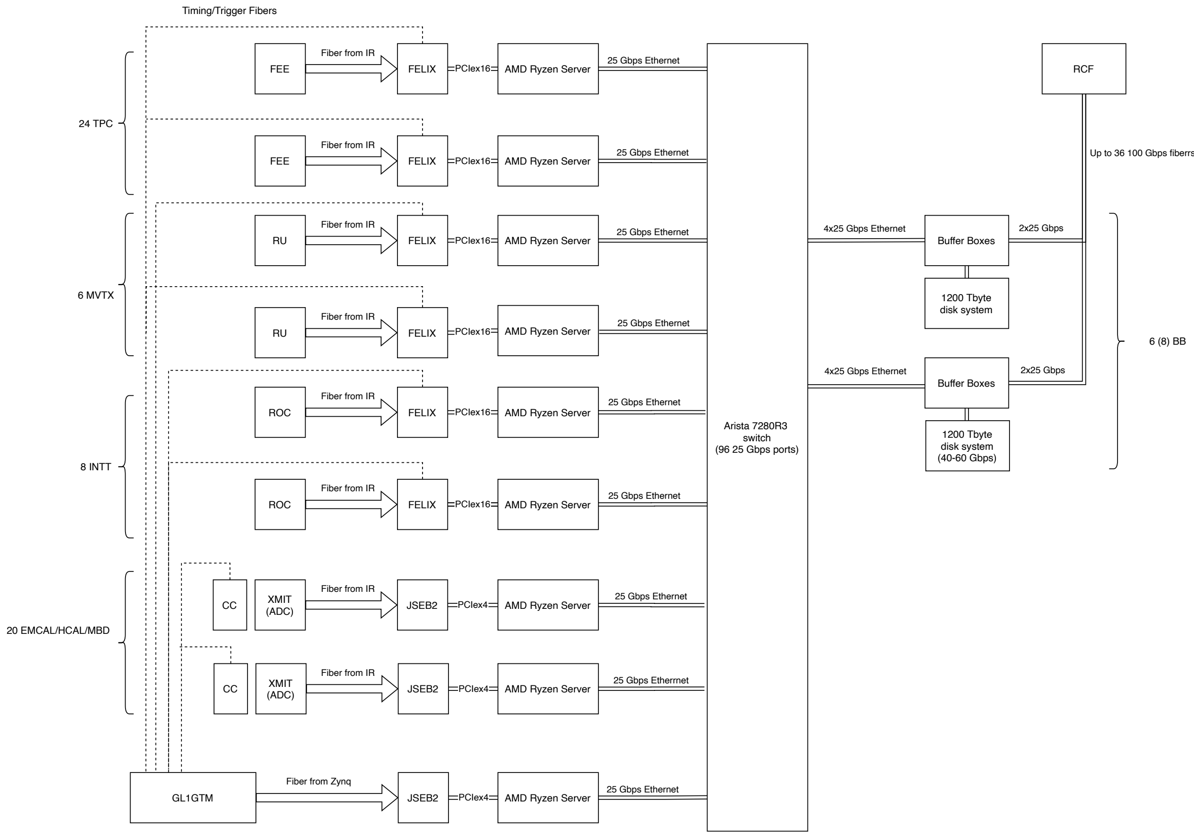

Figure C.3: Block diagram of sPHENIX data acquisition system, showing interfaces to MVTX, INTT, and TPC front end electronics using the ATLAS FELIX interface, and electromagnetic and hadronic calorimeters and Minimum Bias Detector using the DCM2 and JSEB card.

C.1.3 Data Preservation and Data Mining

This upgrade will accumulate a large amount (10–100% of delivered luminosity) of minimum bias polarized $p+p$ data without a trigger bias and with the full sPHENIX tracking capability. Asr RHIC completes its scientific mission at the end of the sPHENIX program, this unique data set would allow future data mining for novel quantum effects such as quantum coherence in particle production. Such future analyses would have the full freedom to define an “event” in the offline software “trigger” that is based on high level objects such as tracklets and final detector alignment and calibrations. These $p+p$ data may be critical for fully understanding the future $e-$ Acollision data at the Electron Ion Collider [41].

C.2 De-Multiplexing the Calorimeter Readout

The sPHENIX data acquisition system is designed to acquire events from the front end electronics at 15 kHz with a livetime of 90% or greater. Custom digitizers on the detector have been designed to transmit data over fiber optic cables to computers in the sPHENIX Rack Room which record data to local fileservers before copying the data to the RACF for archiving and analysis. A block

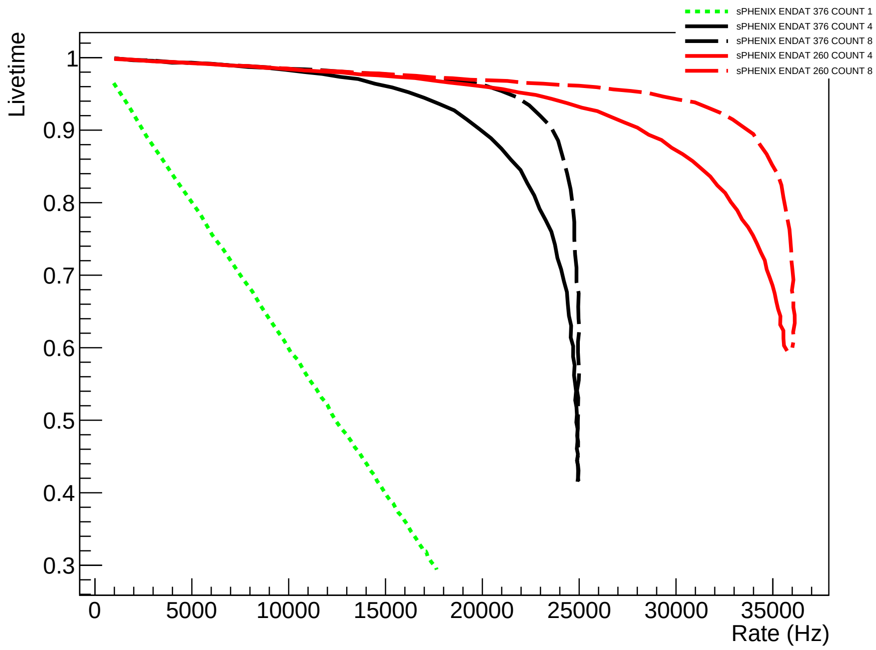

Figure C.4: Livetime as a function of trigger rate for calorimeter digitizers for 1, 4, and 8 event buffering in the front end in the baseline design (black), and with possible future upgrades (red). For comparison, the green line shows the effect of single event buffering, or stop-and-read.

diagram of the system is shown in Figure C.3. The system is designed with high speed links and buffering at several points to achieve the design livetime at a 15 kHz event rate. In the absence of data flow bottlenecks, the livetime is limited by the ADC system used to read out the three calorimeters (EMCal, iHCal and oHCal) and the Minimum Bias Detector.

The ADC system used by the calorimeters uses 60 MHz waveform digitizers to record a fixed number of samples at the time of a Level-1 trigger, which are buffered locally on the detector for 4, and possibly as many as 8, events before serialization and transmission over optical fiber from a digitizer ”XMIT” board to second generation Data Collection Modules (DCM II) — reused from the PHENIX experiment — which zero suppress and re-format the data. The sPHENIX baseline design collects data from three ADC modules (192 channels) to one fiber (by way of the XMIT board), and the time to transmit an event ultimately determines the livetime as a function of event rate. Assuming there are no data transmission bottlenecks downstream which would require throttling the data flow, the transmission time for a single event is designed to be about 40 μsec. Buffering events at the digitizer makes it possible to achieve a livetime greater than 90% with 15 kHz of input triggers, but the livetime decreases as the trigger rate approaches 25 kHz, as shown by the black curves in Figure C.4.

A possible upgrade to the ADC system which could nearly double the rate of recorded events while maintaining the 90% livetime would be to decrease the number ADC modules serialized on one fiber in the electromagnetic calorimeter. Reducing the number of ADC boards per fiber to two would not require more crates on the detector, and would decrease the transmission time to about 28 μsec. The pronounced effect of this *de-multiplexing* is shown by the red curves in Figure C.4.

This upgrade would require 64 additional XMIT boards and eight additional DCM II boards as well as some additional electronics, fibers, and crates to serve them. A rough estimate of the cost is $100–150k in electronics and a similar cost for engineering, for a total cost of about $300k. Due to parts obsolescence and continuing advances in electronics, it might be preferable to design a replacement for the DCM II modules, but it is not practical to consider such a project until the baseline electronics is installed and operating.

Appendix D

Potential Beam Use Proposal 2026–2027

In this appendix we provide details on a potential additional two years of running in 2026–2027 that presents a further return on investment in sPHENIX and also the entire RHIC program. We highlight that if such a window of opportunity arises this would represent the last opportunity for data taking in heavy-ion mode in this energy regime in our lifetime.

D.1 Proposal Summary

The sPHENIX proposal for such a potential window of opportunity is summarized in Table D.1. The two years assume 28 cryo-weeks in each and with a sPHENIX uptime of 80% with detector operations having reached a mature state. The projected luminosities are documented for the years 2026 and 2027 using guidance from C-AD. For completeness, we detail in the cryo-weeks for the potential 2026 and 2027 runs at the end of this Chapter in Section D.4.

We highlight that key upgrades at very modest cost can have a major increase in the physics impact of these additional years of running. Demultiplexing the calorimeter readout increases the Level-1 trigger accept rate to 30 kHz, doubling the rate of calorimeter data events. Increasing the tracking detectors streaming readout to 100% results in an order of magnitude more data than in the 2024–2025 data-taking period. These upgrade options are detailed in Chapter C.

Table D.1: The recorded luminosity (Rec. Lum.) and sampled luminosity (Samp. Lum.) values are for collisions with z-vertex $|z| < 10$ cm.

Year	Species	$\sqrt{s_{NN}}$ [GeV]	Cryo Weeks	Physics Weeks	Rec. Lum. $|z|$ <10 cm	Samp. Lum. $|z|$ <10 cm
2026	$p^{\uparrow}p^{\uparrow}$	200	28	15.5	1.0 pb^{-1} [10 kHz] 80 pb^{-1} [100%-str]	80 pb^{-1}
–	O+O	200	–	2	18 nb^{-1} 37 nb^{-1} [100%-str]	37 nb^{-1}
–	Ar+Ar	200	–	2	6 nb^{-1} 12 nb^{-1} [100%-str]	12 nb^{-1}
2027	Au+Au	200	28	24.5	30 nb^{-1} [100%-str/DeMux]	30 nb^{-1}

D.2 Au+Au and $p+p$ Physics Reach

First, we start with the Au+Au increased physics reach. In Table D.2 we compare directly the Au+Au recorded and sampled luminosities from the three runs in 2023, 2025, and the potential opportunity in 2027. The upgrades enable a doubling of the Au+Au data set to 30 nb^{-1} or equivalently 200 billion Au+Au events. These events will serve as a permanent archive of Au+Au data, to be mined for any future analysis once RHIC is no longer running heavy ions. There are no trigger biases or selections that would preclude any analysis within the acceptance and performance parameters of sPHENIX.

The impact on the polarized $p+p$ data set is even more substantial, not only for the heavy ion program but also for studies of spin-dependent QCD. The comparison of running $p+p$ in 2024 and 2026 is shown in Table D.3. The striking gain is in the 80 pb^{-1} recorded with the tracking detectors via 100%-str mode, more than a factor of ten over the previous data set. There are many measurements, particularly in the heavy-flavor and transverse spin (cold QCD) arena where selective physics triggers are not available and thus the $p+p$ measurements are the statistically limiting factor in the Au+Au-to-$p+p$ comparisons. This enormous data set, with an additional 130 pb^{-1} of data samples for both calorimetric jet and tracking-based measurements, represents an immediate opportunity to advance our precision physics knowledge and to create a permanent archive of data from RHIC.

The substantial increase in statistics translates into ultra-precise measurements of basic observables and the enabling of highly differential observables. Here we show a subset of example projection plots. Figure D.1 (left) shows the improvement in statistical precision for direct photon, jet, and

Table D.2: Summary of Au+Au at 200 GeV running in the sPHENIX Beam Use Proposal. The recorded luminosity (Rec. Lum.) and first sampled luminosity (Samp. Lum.) values are for collisions with z-vertex $|z| < 10$ cm.

Year	Species	$\sqrt{s_{NN}}$ [GeV]	Cryo Weeks	Physics Weeks	Rec. Lum. $|z| <10$ cm	Samp. Lum. $|z| <10$ cm
2023	Au+Au	200	24 (28)	9 (13)	3.7 (5.7) nb^{-1}	4.5 (6.9) nb^{-1}
2025	Au+Au	200	24 (28)	20.5 (24.5)	13 (15) nb^{-1}	21 (25) nb^{-1}
2027	Au+Au	200	28	24.5	30 nb^{-1} [100%-str/DeMux]	30 nb^{-1}

Table D.3: Summary of p+p at 200 GeV running in the sPHENIX Beam Use Proposal. The recorded luminosity (Rec. Lum.) and sampled luminosity (Samp. Lum.) values are for collisions with z-vertex $|z| < 10$ cm.

Year	Species	$\sqrt{s_{NN}}$ [GeV]	Cryo Weeks	Physics Weeks	Rec. Lum. $|z| <10$ cm	Samp. Lum. $|z| <10$ cm
2024	$p^{\uparrow}p^{\uparrow}$	200	24 (28)	12 (16)	0.3 (0.4) pb^{-1} [5 kHz] 4.5 (6.2) pb^{-1} [10%-str]	45 (62) pb^{-1}
2026	$p^{\uparrow}p^{\uparrow}$	200	28	15.5	1.0 pb^{-1} [10 kHz] 80 pb^{-1} [100%-str]	80 pb^{-1}

charged hadron nuclear modification factor R$_{AA}$ as a function of p_T in 0–10% central Au+Au collisions. The higher luminosity, particularly at high-p_T where underlying event backgrounds are low, will enable a precision decomposition of these jet events. Figure D.1 (right) shows the statistical precision for the "golden-channel" photon + jet distribution. The precision is sufficient that one can then further dissect these events and look for medium response opposite the photon in selections of $x_{J\gamma}$. Another example of a statistically-driven measurement is the azimuthal anisotropy of high p_T probes. Figure D.2 shows the statistical uncertainties for jets with $p_T > 40$ GeV as a function of angle relative to the second-order reaction plane. The precision measurements with Year 4–5 (2026–2027) data included will enable a key constraint on jet quenching calculations embedded in a realistic hydrodynamic expanding background.

The Upsilon measurement is another case where additional precision will enable more differential observations. Figure D.3 (left) shows the increased statistical accuracy for the centrality dependence with the added Year 4-5 (2026-2027) data. Figure D.3 (right) shows the improvement in precision

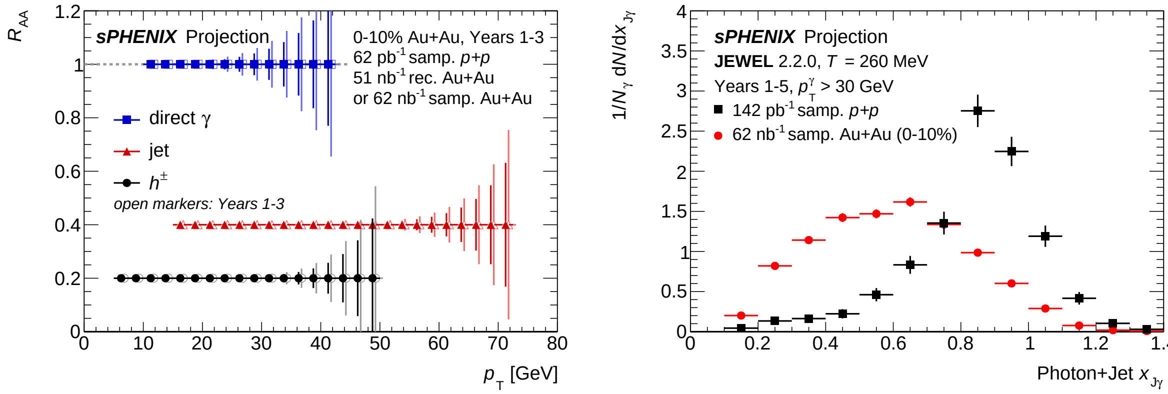

Figure D.1: (left) Nuclear modification factor R_{AA} in 0–10% central Au+Au collisions for direct photons, jets, and charged hadrons as a function of p_T. Shown are the statistical uncertainties from Year 1–3 (2023–2025) running compared with including the additional Year 4–5 (2026–2027) running. (right). Statistical precision for $x_{J\gamma}$ in photon + jet events from additional Year 4–5 (2026–2027) running.

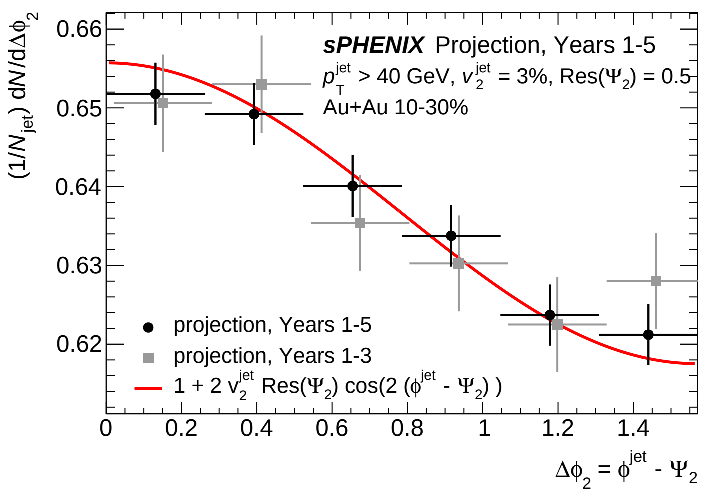

Figure D.2: Statistical projections for the jet yield as a function of the azimuthal distance from the event plane in 10–30% Au+Au events.

for the transverse momentum dependence in the 0–10% most central collisions. Examples of measurements for which the higher luminosity would be valuable are the rapidity dependence for the Υ(1S) and Υ(2S), and correlations measurements, such as azimuthal anisotropies.

The statistical gain from the 2026–2027 data would be beneficial for rare heavy-flavor observables, in particular for exclusive decay channels, HF flow and asymmetries. As shown in Figure D.4, a clean separation of the v_1 for D^0 and $\bar{D}^0$ is expected summing five years of Au+Au data, which would provide quantitative access to the initial magnetic field in heavy-ion collisions [42]. With 100% streaming data acquisition, the D^0 statistics and the uncertainty for the D^0 spin asymmetry A_N are dramatically improved in the polarized p+p collisions as shown in Figure D.5, which provides a strong constraint on the amplitude and p_T dependence of tri-gluon correlations in the

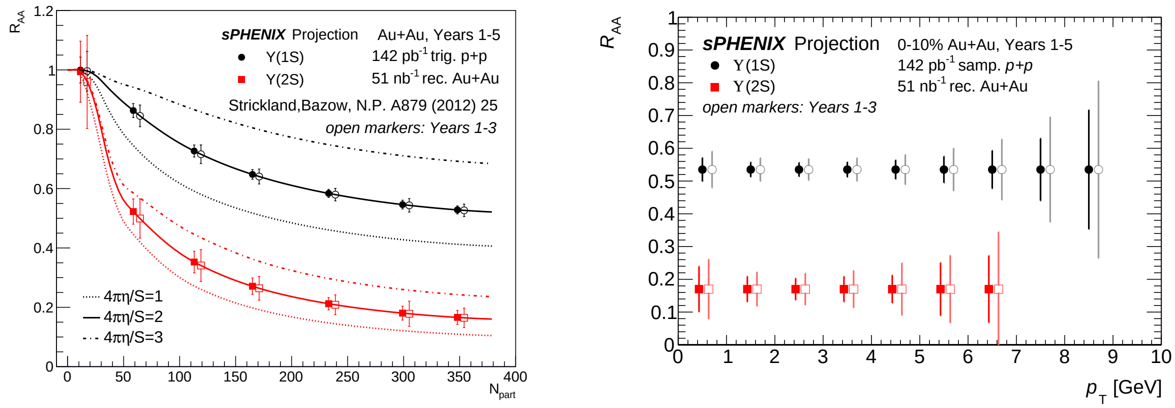

Figure D.3: sPHENIX projected statistical uncertainties, including from background subtraction contributions, for the Upsilon nuclear modification factors as a function of centrality (left) and p_T (right) in the proposed three-year (2023–2025) run plan and then compared with the improved precision adding projected data from 2026–2027.

proton. The collaboration is also studying the viability of full reconstruction of exclusive decay channels such as B_s meson that would provide new information on the strange enhancement and hadronization with the tagging of heavy bottom quark.

Finally, the size of the recorded Au+Au dataset along with the broad capabilities of sPHENIX will allow the community to continue to produce a variety of imaginative and expansive measurements in the years after RHIC has completed data-taking. These include new measurements of correlations and fluctuations, the chiral magnetic effect, the production of soft photons via conversion methods, and others not yet envisioned.

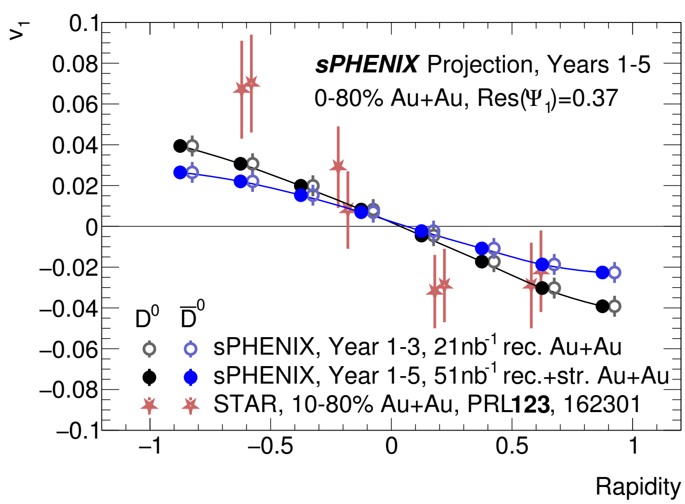

Figure D.4: Projection for direct flow of D^0 and $\bar{D}^0$ mesons (black and blue data points), which is compared with recent results from STAR [43] (red points) and calculations combining effects from the tilted geometry [44] and the initial EM fields [42] (curves).

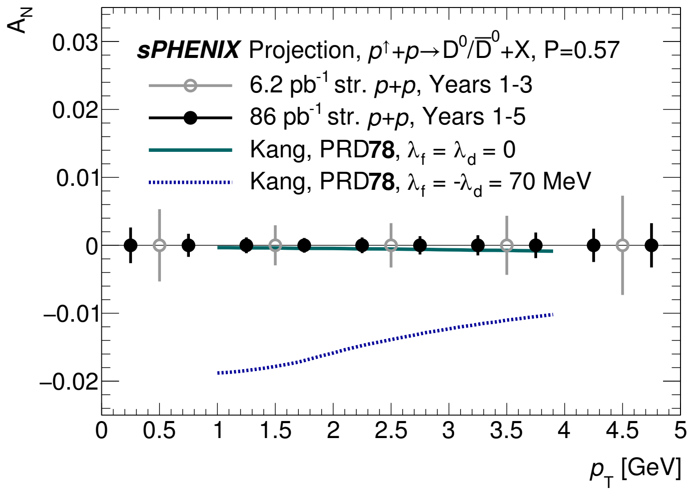

Figure D.5: Statistical projections of transverse spin asymmetry for the D^0 mesons for five years data taking, a dramatic improvement over the initial three-year data discussed in Section 4.4.

D.3 O+O and Ar+Ar Physics Reach

The RHIC program has a 100% track record of learning new physics and gaining insights from every novel nuclear species combinations put into collision. It is a testament to the facility and the constant improvements, including the EBIS source, that have been the lifeblood of the machine. An opportunity to run smaller symmetric collision species, such as O+O and Ar+Ar, is essentially guaranteed to provide key insights and resolve some key outstanding puzzles in the field. Here we outline one possible plan for small systems running. However, the particular running plan in 2026 could ultimately involve different combinations of small nuclei, depending on the discoveries made using 2023–2025 sPHENIX data, those made during the concurrent LHC Run 3 which will potentially include O+O collisions, and developments in theory during that time.

A major open question in the field and an associated major puzzle relates to jet quenching or the lack thereof in small systems, for example p+Au at RHIC and p+Pb at the LHC. Despite a wealth of evidence for collectivity [31], described by hydrodynamics in these small systems, the p_T distribution of charged hadrons, reconstructed jets, and open heavy-flavor hadrons appears nearly unmodified, i.e. $\mathrm{R}_{pA} = 1$ within uncertainties. Is there a minimum medium size or lifetime requires for jet quenching phenomena? Does such a minimum value relate to hard struck quarks and gluons having a formation time before scattering in medium or having coherence effects? These are fundamental questions that are needed to fully understand the physics of small systems and to bridge the divide between small and large systems.

The associated major puzzle is that at the LHC in p+Pb collisions there is a definite azimuthal anisotropy for charged hadrons up to $p_T \approx 50$ GeV [38], and D mesons and their decay leptons are observed to have an azimuthal anisotropy as well in $p+A$ and even $p+p$ collisions. In A+A collisions, the high-p_T v_2 is interpreted as differential jet quenching, which would seem impossible in small systems if there is no indication of jet quenching in the nuclear modification factor.

sPHENIX will extend these measurements as part of the p+Au running in 2024 as discussed in Section 4.4.

In principle one can use peripheral Au+Au or Pb+Pb collisions to map out these observables and bridge the divide between large and small systems. However, there are substantial event selection biases that have recently been shown to have caused $R_{AA} < 1$ in peripheral A+A collisions at RHIC and the LHC [45]. Correcting for these biases is challenging particularly if one is teasing out modest modifications in the p_T distribution of order 10–20%. One solution to this problem is to run smaller symmetric nuclear collision species. One can use minimum bias events where there is no event selection bias, and one can also use selected high-multiplicity events where the bias is in the opposite direction to that in Au+Au and thus one can test whether one can correct out this bias.

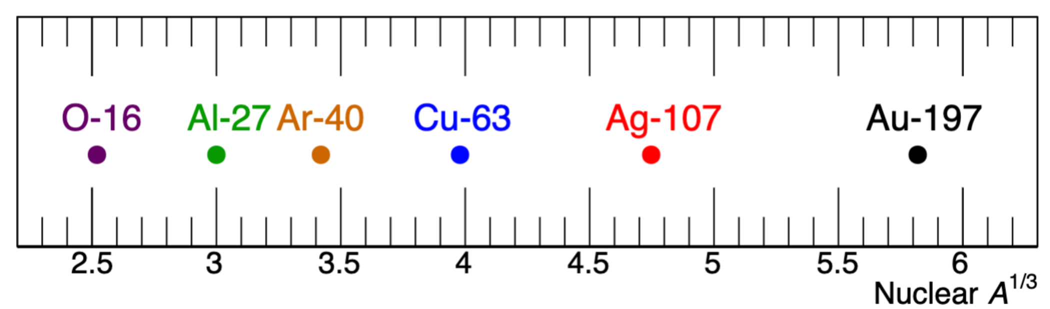

Figure D.6: Various nuclei plotted as a function of $A^{1/3}$.

What is the optimum nuclear collisions species and for how many weeks should one run to collect the necessary data set? Figure D.6 shows the nuclear thickness as it scales with $A^{1/3}$ for different potential nuclei. Monte Carlo Glauber and direct photon NLO rates are combined with C-AD luminosity projections to plot the number of jets and direct photons that can be measured by sPHENIX per week of running as a function of the number of binary collisions N_{coll}, as shown in Figure D.7.

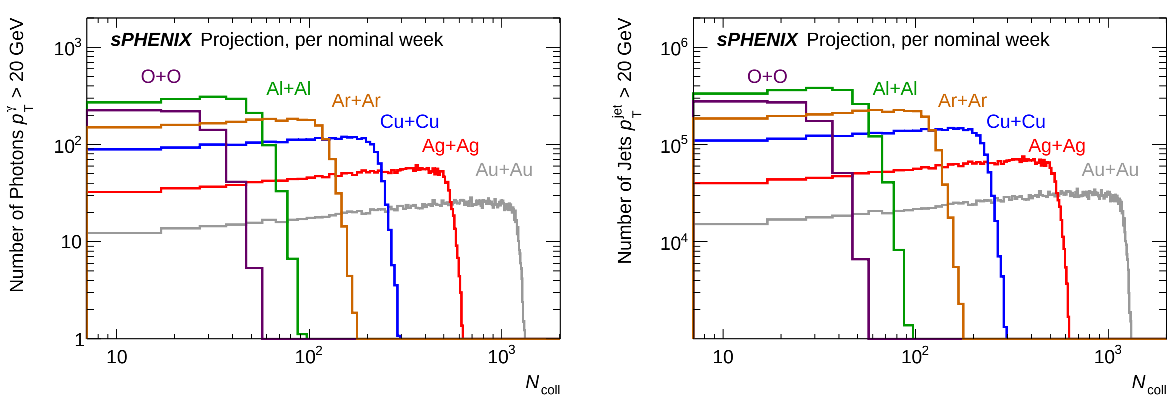

Figure D.7: Number of direct photons (left) and jets (right) with $p_T > 20$ GeV measurable by sPHENIX per nominal week of delivered luminosity as a function of the number of binary collisions.

An optimum balance of system size and running time is closely matched by running two weeks of physics data taking for O+O and Ar+Ar. Using projections from C-AD, even during this short

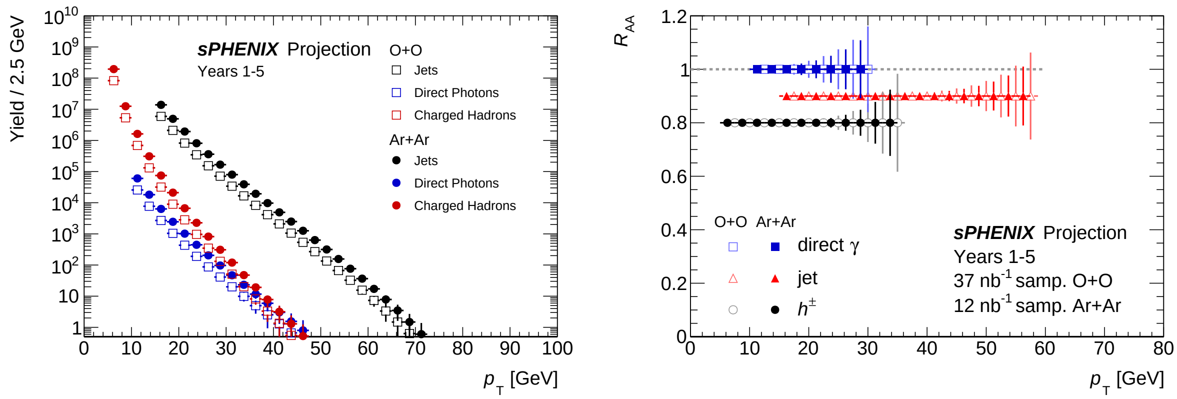

Figure D.8: Projected total yields (left) and R_{AA} (right) for jets, photons, and charged hadrons in O+O and Ar+Ar events taken during a potential sPHENIX run in 2026.

running period, one can measure direct photons beyond 25 GeV and jets out beyond 50 GeV as shown in Figure D.8. The direct photon measurement in particular enables confirmation of minimum bias A-scaling of the cross section as well as any corrections to bias factors in multiplicity-selected events.

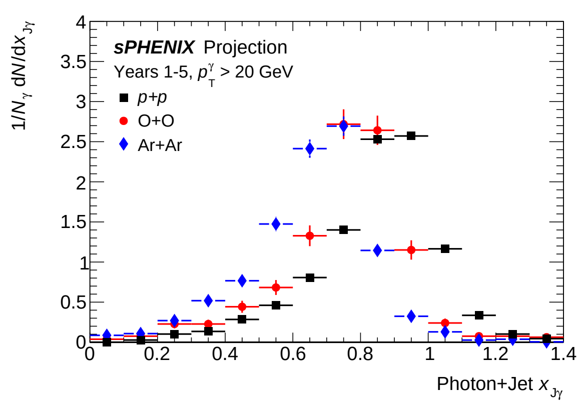

Figure D.9: Projected jet-to-photon p_T balance distributions for $p_T^{\gamma} > 20$ GeV in $p+p$, O+O, and Ar+Ar events taken during a potential sPHENIX run in 2026.

This sample will also enable differential measurements of many quantities. For example, Figure D.9 shows projected $x_{J\gamma}$ distributions for $p_T^{\gamma} > 20$ GeV, for which there will be 800 and 1 900 events in O+O and Ar+Ar data, respectively. The projection shows that there will be sufficient data to make a compelling measurement of γ-tagged energy loss in these small symmetric systems. As a note, the projection includes very low values of $x_{J\gamma} < 0.4$ at which jet measurements may not be feasible. However, the physics effect is primarily at high $x_{J\gamma}$ since the magnitude of energy loss is expected to be small, and one could use photon–hadron correlations to explore the very low-p_T physics.

Figure D.10 (left) shows a projection for the v_2 for charged hadrons as a function of p_T for both O+O and Ar+Ar. sPHENIX will have sufficient reach to measure out to $p_T \sim 25$ GeV. In large A+A systems, a non-zero v_2 in this kinematic region, which is far outside the low-p_T region governed by hydrodynamic expansion, is conventionally understood to arise from a path-length dependent jet

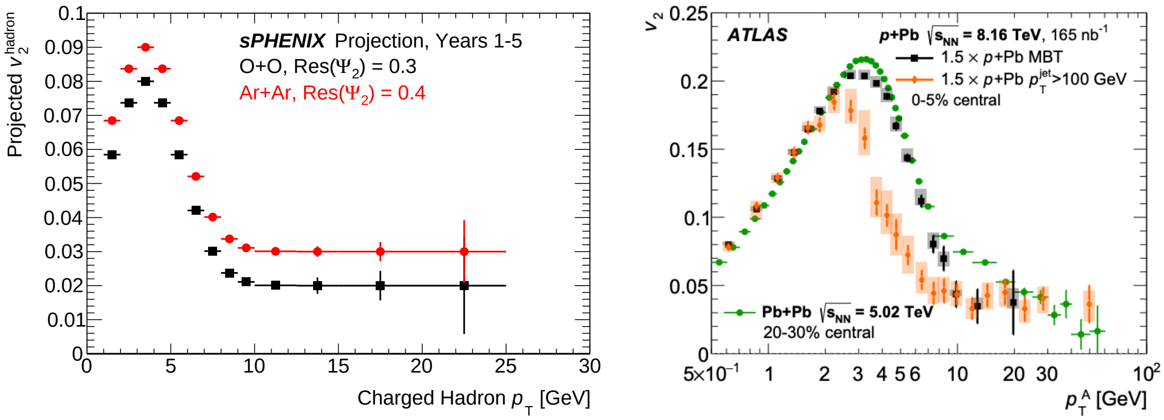

Figure D.10: (Left) Statistical projection for charged hadron v_2 in O+O and Ar+Ar data as a function of p_{T}. (Right) ATLAS high-p_T v_2 in p+Pb and Pb+Pb collisions at the LHC. [38]

energy loss. However, recent results at the LHC, shown in Figure D.10 (right), show that a small, non-zero v_2 is observed even in p+Pb collisions out to 50 GeV, despite no significant energy loss observed in other measurements. Since sPHENIX will be able to make simultaneous measurements of the v_2 and the R_{AA} with high precision in both O+O and Ar+Ar, we can map out the physics of systems with sizes between the p+A and A+A in detail.

Additionally, the related puzzle of heavy-flavor anisotropies in p+p and p+A but with $\mathrm{R}_{pA} \approx 1$ can be tested in these small systems. As shown in Figure D.11, a large minimum bias sample for prompt D^0 can be detected allowing simultaneously high precision measurement of its nuclear modification and v_2. Similar observables can be further extends to other heavy-flavor channels, such as the non-prompt D^0 mesons which provide a window into the heavier of the heavier b-quark in these collision systems. Measurements in O+O and Ar+Ar of heavy-flavor R_{AA} and v_2 are a key part of understanding the physics in these small systems. There are theoretical proposals that the azimuthal anisotropy in small systems for heavy-flavor hadrons and quarkonia comes from initial-state Color Glass Condensate effects. However, this is challenged by the idea that the heavy-flavor particles are correlated with all bulk low-p_T particles that are described by hydrodynamics. These data will provide further tests of any models working towards solving the small system HF puzzle.

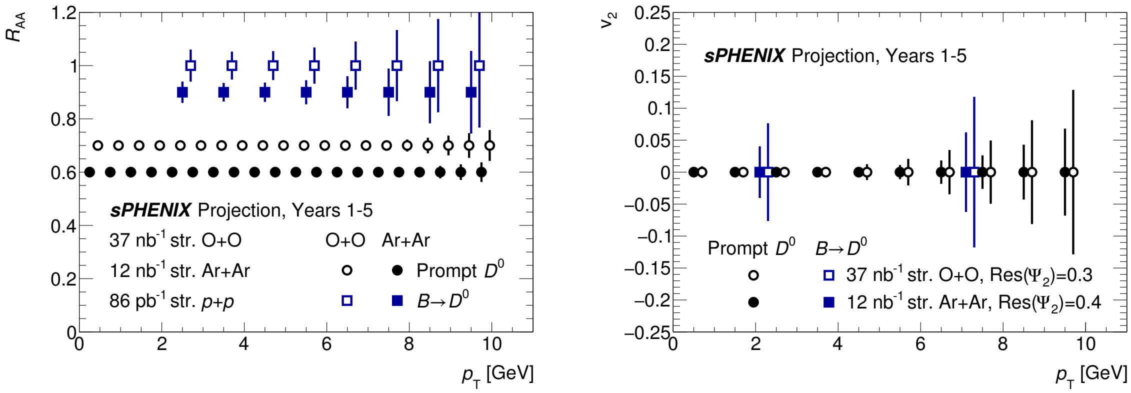

Figure D.11: Projection for R_{AA} (left) and v_2 (right) for prompt (black) and non-prompt (blue) D^0 production in the M.B. O+O (open marker) and Ar+Ar (filled marker) collisions.

D.4 Cryo-Week Details

For completeness, we detail the 28 cryo-weeks of potential running in 2026 and 2027 in Table D.4 and Table D.5 respectively.

Weeks	Designation
0.5	Cool Down from 50 K to 4 K
2.0	Set-up mode 1 ($p^{\uparrow}p^{\uparrow}$ at 200 GeV)
0.5	Ramp-up mode 1 (8 h/night for experiment)
15.5	Data taking mode 1 ($p^{\uparrow}p^{\uparrow}$ Physics)
2.0	Set-up mode 2 (O+O at 200 GeV)
0.5	Ramp-up mode 2 (8 h/night for experiment)
2.0	Data taking mode 2 (O+O Physics)
2.0	Set-up mode 3 (Ar+Ar at 200 GeV)
0.5	Ramp-up mode 3 (8 h/night for experiment)
2.0	Data taking mode 3 (Ar+Ar Physics)
0.5	Controlled refrigeration turn-off
28.0	Total cryo-weeks

Table D.4: Year 2026 run plan for 28 cryo-weeks with $p^{\uparrow}p^{\uparrow}$, O+O, and Ar+Ar 200 GeV collisions.

Weeks	Designation
0.5	Cool Down from 50 K to 4 K
2.0	Set-up mode 1 (Au+Au at 200 GeV)
0.5	Ramp-up mode 1 (8 h/night for experiments)
24.5	Data taking mode 1 (Physics)
0.5	Controlled refrigeration turn-off
28.0	Total cryo-weeks

Table D.5: Year 2027 run plan for 28 cryo-weeks with Au+Au 200 GeV collisions.

Bibliography

[1] Yasuyuki Akiba et al. The Hot QCD White Paper: Exploring the Phases of QCD at RHIC and the LHC. 2 2015. arXiv:1502.02730. 1.1

[2] Ani Aprahamian et al. Reaching for the horizon: The 2015 long range plan for nuclear science. 10 2015. 1.1

[3] sPHENIX Technical Design Report. 5 2019. URL: https://indico.bnl.gov/event/7081/. 1.1

[4] sPHENIX preConceptual Design Report. 10 2015. 1.1

[5] A. Adare et al. An Upgrade Proposal from the PHENIX Collaboration. 1 2015. arXiv:1501.06197. 4.1

[6] M. L. Miller, K. Reygers, S. J. Sanders, and P. Steinberg. Glauber modeling in high energy nuclear collisions. *Ann. Rev. Nucl. Part. Sci.*, 57:205–243, 2007. doi:10.1146/annurev.nucl.57.090506.123020. 4.1

[7] Raghav Kunnawalkam Elayavalli and Korinna Christine Zapp. Simulating V+jet processes in heavy ion collisions with JEWEL. *Eur. Phys. J. C*, 76(12):695, 2016. arXiv:1608.03099, doi:10.1140/epjc/s10052-016-4534-6. 4.1

[8] Georges Aad et al. Measurements of azimuthal anisotropies of jet production in Pb+Pb collisions at $\sqrt{s_{NN}} = 5.02$ TeV with the ATLAS detector. 11 2021. arXiv:2111.06606. 4.1

[9] Jaroslav Adam et al. Azimuthal anisotropy of charged jet production in $\sqrt{s_{\mathrm{NN}}}$ = 2.76 TeV Pb-Pb collisions. *Phys. Lett. B*, 753:511–525, 2016. arXiv:1509.07334, doi:10.1016/j.physletb.2015.12.047. 4.1

[10] Albert M Sirunyan et al. First measurement of large area jet transverse momentum spectra in heavy-ion collisions. *JHEP*, 05:284, 2021. arXiv:2102.13080, doi:10.1007/JHEP05(2021)284. 4.1

[11] M. Strickland and D. Bazow. Thermal bottomonium suppression at RHIC and LHC. *Nucl. Phys.*, A879:25–58, 2012. arXiv:1112.2761, doi:10.1016/j.nuclphysa.2012.02.003. 4.5

[12] S. S. Cao, G.Y. Qin, and S. A. Bass. Energy loss, hadronization and hadronic interactions of heavy flavors in relativistic heavy-ion collisions. *Phys. Rev.*, C92:024907, 2015. doi:10.1103/PhysRevC.92.024907. 4.6, 4.7

[13] Min He, Rainer J. Fries, and Ralf Rapp. Heavy-Quark Diffusion and Hadronization in Quark-Gluon Plasma. *Phys. Rev.*, C86:014903, 2012. `doi:10.1103/PhysRevC.86.014903`. 4.6, 4.7

[14] T. Song, H. Berrehrah, J. M. Torres-Rincon, L. Tolos, D. Cabrera, W. Cassing, and E. Bratkovskaya. Single electrons from heavy-flavor mesons in relativistic heavy-ion collisions. *Phys. Rev.*, C96:014905, 2017. 4.6, 4.7

[15] J.C. Xu, J.F. Liao, and M. Gyulassy. Bridging soft-hard transport properties of quark-gluon plasmas with cujet3.0. *JHEP*, 1602:169, 2016. `doi:10.1007/JHEP02(2016)169`. 4.6

[16] Jinrui Huang, Zhong-Bo Kang, and Ivan Vitev. Inclusive b-jet production in heavy ion collisions at the LHC. *Phys. Lett.*, B726:251–256, 2013. `arXiv:1306.0909`, `doi:10.1016/j.physletb.2013.08.009`. 4.6

[17] Weiyao Ke, Xin-Nian Wang, Wenkai Fan, and Steffen Bass. Study of heavy-flavor jets in a transport approach. 8 2020. `arXiv:2008.07622`. 4.6

[18] L. Adamczyk et al. Measurement of D^0 Azimuthal Anisotropy at Midrapidity in Au+Au Collisions at $\sqrt{s_{NN}}$=200 GeV. *Phys. Rev. Lett.*, 118(21):212301, 2017. `arXiv:1701.06060`, `doi:10.1103/PhysRevLett.118.212301`. 4.7

[19] Guy D. Moore and Derek Teaney. How much do heavy quarks thermalize in a heavy ion collision? *Phys. Rev.*, C71:064904, 2005. `arXiv:hep-ph/0412346`, `doi:10.1103/PhysRevC.71.064904`. 4.3

[20] Santosh K. Das, Francesco Scardina, Salvatore Plumari, and Vincenzo Greco. Heavy-flavor in-medium momentum evolution: Langevin versus Boltzmann approach. *Phys. Rev.*, C90:044901, 2014. `arXiv:1312.6857`, `doi:10.1103/PhysRevC.90.044901`. 4.3

[21] Zhong-Bo Kang, Jared Reiten, Ivan Vitev, and Boram Yoon. Light and heavy flavor dijet production and dijet mass modification in heavy ion collisions. *Phys. Rev. D*, 99(3):034006, 2019. `arXiv:1810.10007`, `doi:10.1103/PhysRevD.99.034006`. 4.8, 4.3

[22] X. Chen et al. sPHENIX simulation Note sPH-HF-2017-002: D^0-meson and B^+-meson production in Au+Au collisions at $\sqrt{s_{NN}} = 200$ GeV for sPHENIX. 2017. URL: `http://portal.nersc.gov/project/star/dongx/sPHENIX/sPH-HF-2017-002-v1.pdf`. 4.3

[23] sPHENIX simulation Note sPH-HF-2017-001: Heavy Flavor Jet Simulation and Analysis. 2017. URL: `https://indico.bnl.gov/event/3959/`. 4.3

[24] Hai Tao Li and Ivan Vitev. Inverting the mass hierarchy of jet quenching effects with prompt b-jet substructure. *Phys. Lett. B*, 793:259–264, 2019. `arXiv:1801.00008`, `doi:10.1016/j.physletb.2019.04.052`. 4.3, 4.9

[25] Jaroslav Adam et al. First Measurement of Λ_c Baryon Production in Au+Au Collisions at $\sqrt{s_{NN}}$=200 GeV. *Phys. Rev. Lett.*, 124(17):172301, 2020. `arXiv:1910.14628`, `doi:10.1103/PhysRevLett.124.172301`. 4.3, 4.10

[26] Zhong-Bo Kang, Jian-Wei Qiu, Werner Vogelsang, and Feng Yuan. Accessing tri-gluon correlations in the nucleon via the single spin asymmetry in open charm production. *Phys. Rev. D*, 78:114013, 2008. `arXiv:0810.3333`, `doi:10.1103/PhysRevD.78.114013`. 4.11, C.1.1

[27] Leszek Adamczyk et al. Azimuthal transverse single-spin asymmetries of inclusive jets and charged pions within jets from polarized-proton collisions at $\sqrt{s} = 500$ GeV. *Phys. Rev. D*, 97(3):032004, 2018. `arXiv:1708.07080`, `doi:10.1103/PhysRevD.97.032004`. 4.4.1

[28] L. Adamczyk et al. Transverse spin-dependent azimuthal correlations of charged pion pairs measured in $p^{\uparrow}$+p collisions at $\sqrt{s}$ = 500 GeV. *Phys. Lett. B*, 780:332–339, 2018. `arXiv:1710.10215`, `doi:10.1016/j.physletb.2018.02.069`. 4.4.1

[29] C. Aidala et al. Nuclear Dependence of the Transverse Single-Spin Asymmetry in the Production of Charged Hadrons at Forward Rapidity in Polarized $p + p$, p+Al, and p+Au Collisions at $\sqrt{s_{_{NN}}} = 200$ GeV. *Phys. Rev. Lett.*, 123(12):122001, 2019. `arXiv:1903.07422`, `doi:10.1103/PhysRevLett.123.122001`. 4.4.2

[30] Jaroslav Adam et al. Comparison of transverse single-spin asymmetries for forward π^0 production in polarized pp, pAl and pAu collisions at nucleon pair c.m. energy $\sqrt{s_{\mathrm{NN}}} = 200$ GeV. *Phys. Rev. D*, 103(7):072005, 2021. `arXiv:2012.07146`, `doi:10.1103/PhysRevD.103.072005`. 4.4.2

[31] James L. Nagle and William A. Zajc. Small System Collectivity in Relativistic Hadronic and Nuclear Collisions. *Ann. Rev. Nucl. Part. Sci.*, 68:211–235, 2018. `arXiv:1801.03477`, `doi:10.1146/annurev-nucl-101916-123209`. 4.4.4, D.3

[32] C. Aidala et al. Measurements of Multiparticle Correlations in $d+$Au Collisions at 200, 62.4, 39, and 19.6 GeV and $p+$Au Collisions at 200 GeV and Implications for Collective Behavior. *Phys. Rev. Lett.*, 120(6):062302, 2018. `arXiv:1707.06108`, `doi:10.1103/PhysRevLett.120.062302`. 4.4.4

[33] C. Aidala et al. Creation of quark–gluon plasma droplets with three distinct geometries. *Nature Phys.*, 15(3):214–220, 2019. `arXiv:1805.02973`, `doi:10.1038/s41567-018-0360-0`. 4.4.4

[34] U. A. Acharya et al. Kinematic dependence of azimuthal anisotropies in $p + Au$, $d + Au$, and $^3He + Au$ at $\sqrt{s}_{NN} = 200$ GeV. *Phys. Rev. C*, 105(2):024901, 2022. `arXiv:2107.06634`, `doi:10.1103/PhysRevC.105.024901`. 4.4.4

[35] A. M. Sirunyan et al. Elliptic flow of charm and strange hadrons in high-multiplicity pPb collisions at $\sqrt{s_{_{\mathrm{NN}}}} = 8.16$ TeV. *Phys. Rev. Lett.*, 121(8):082301, 2018. `arXiv:1804.09767`, `doi:10.1103/PhysRevLett.121.082301`. 4.4.4, 4.15

[36] Jaroslav Adam et al. D-meson production in p-Pb collisions at $\sqrt{s_{\mathrm{NN}}}$ =5.02 TeV and in pp collisions at $\sqrt{s}$ =7 TeV. *Phys. Rev. C*, 94(5):054908, 2016. `arXiv:1605.07569`, `doi:10.1103/PhysRevC.94.054908`. 4.4.4

[37] Georges Aad et al. Measurement of azimuthal anisotropy of muons from charm and bottom hadrons in pp collisions at $\sqrt{s} = 13$ TeV with the ATLAS detector. *Phys. Rev. Lett.*, 124(8):082301, 2020. `arXiv:1909.01650`, `doi:10.1103/PhysRevLett.124.082301`. 4.4.4

[38] Georges Aad et al. Transverse momentum and process dependent azimuthal anisotropies in $\sqrt{s_{\mathrm{NN}}} = 8.16$ TeV p+Pb collisions with the ATLAS detector. *Eur. Phys. J. C*, 80(1):73, 2020. `arXiv:1910.13978`, `doi:10.1140/epjc/s10052-020-7624-4`. 4.4.4, D.3, D.10

[39] sPH-COMP-2019-001: sPHENIX computing plan. 2019. URL: `https://indico.bnl.gov/event/6659/`. C.1.1

[40] Yuji Koike and Shinsuke Yoshida. Probing the three-gluon correlation functions by the single spin asymmetry in $p^{\uparrow}p \to DX$. *Phys. Rev. D*, 84:014026, 2011. `arXiv:1104.3943`, `doi:10.1103/PhysRevD.84.014026`. C.1.1

[41] A. Accardi et al. Electron Ion Collider: The Next QCD Frontier - Understanding the glue that binds us all. 2012. `arXiv:1212.1701`. C.1.3

[42] Gabriele Coci, Lucia Oliva, Salvatore Plumari, Santosh Kumar Das, and Vincenzo Greco. Direct flow of heavy mesons as unique probe of the initial Electro-Magnetic fields in Ultra-Relativistic Heavy Ion collisions. *Nucl. Phys. A*, 982:189–191, 2019. `arXiv:1901.05394`, `doi:10.1016/j.nuclphysa.2018.08.020`. D.2, D.4

[43] Jaroslav Adam et al. First Observation of the Directed Flow of D^0 and $\overline{D^0}$ in Au+Au Collisions at $\sqrt{s_{\rm NN}}$ = 200 GeV. *Phys. Rev. Lett.*, 123(16):162301, 2019. `arXiv:1905.02052`, `doi:10.1103/PhysRevLett.123.162301`. D.4

[44] Sandeep Chatterjee and Piotr Bożek. Large directed flow of open charm mesons probes the three dimensional distribution of matter in heavy ion collisions. *Phys. Rev. Lett.*, 120(19):192301, 2018. `arXiv:1712.01189`, `doi:10.1103/PhysRevLett.120.192301`. D.4

[45] Constantin Loizides and Andreas Morsch. Absence of jet quenching in peripheral nucleus–nucleus collisions. *Phys. Lett. B*, 773:408–411, 2017. `arXiv:1705.08856`, `doi:10.1016/j.physletb.2017.09.002`. D.3